Dear referee,

Thank you very much for reviewing the manuscript and providing comments. Your comments are helpful for improving the manuscript. In the following, we address all comments point-by-point.

> ***Comment 1****: Add the word "simulated" or something similar to the title. I know that with the dates it is clear that this is enough an actual 439 year dataset of measured data, but save the reader from momentary excitement at a record being found that goes back that far. What is the target audience for this paper? I think the goals of the paper need to be more clearly stated.*

Answer:

We added the "simulated" before the word "daily" as follow:
"A 439-year simulated daily discharge dataset (1861-2299) for the upper Yangtze River, China"
We added one sentence to abstract:
"The long-term daily discharge dataset can be used in the international context and water management, e.g. in the framework of Inter-Sectoral Impact Model Intercomparison Project (ISIMIP) by providing clue to what extent human-induced climate change could impact streamflow and streamflow trend in future."

> ***Comment 2****: Who do you envision using this dataset? For what potential purposes?*

Answer:

In order to respond the simulation protocol of the Inter-Sectoral Impact Model Intercomparison Project (ISIMIP2b: https://www.isimip.org/protocol/#isimip2b). This dataset is used widely for cross-sectoral projections and can also be applied to assess changes in river discharge attributable to anthropogenic climate change.

> ***Comment 3****: In the goals for ESSD, does this paper provide "original research data"? I am not a modeler and thus am not up to date on whether any of the methods presented are new or novel.*

Answer:

We provided the outputs simulated by four hydrological models and will upload the original research data and simulated data as much as possible. The novelty of our manuscript is quite clear. We use multiple hydrological models, which were driven by multiple GCMs under scenarios with and without anthropogenic climate change effects, to deduce the longer discharge series over 400 years.

Comment 4: Figure 1 is not referenced anywhere in the paper

Answer:

We have added a reference to Fig. 1 in the section “Study area": Location of the Cuntan hydrological station, 311 GCM grids, meteorological stations and spatial distribution of the land use and soil types in the upper Yangtze River basin are shown in Fig. 1.

***Comment 5**: Make it clear what the period of daily measured discharge is.*

Answer:

“The daily discharge record at the Cuntan station in the upper Yangtze River is available for 1970 - 1999 from the China Hydrological Yearbook - Yangtze. The rest of daily record for periods 1939 - 1969 and 2000 - 2012 is collected from the Changjiang Water Resources Commission, Ministry of Water Resources in China.” (Section 3.2, page 4, line 11).

1. Introduction

***Comment 6**: First sentence of the intro should be stronger, don't start with “with”.*

Answer:

We modified the sentence in the revised paper:
“Global warming is the long-term rise in average temperature of the earth's climate system. Warming temperature alters global water circulation processes and could significantly influence the sustainability of society and economy (Jung et al., 2011). The variation in water resource availability in the context of global warming is acknowledged as a focus of many international research projects (Stagl et al., 2016; Raman et al., 2018; Maisa et al., 2019). The long-term accurate (as much as possible) daily discharge time series are crucial for in-depth understanding of the changes in streamflow, and they are needed for subsequent climate change impact studies. However, discharge is monitored usually only for short observational periods in most river basins.”

***Comment 7:** Line 8 of the intro, don't start with “To date”*

Answer:

We revised the sentence as:
“For generation of the long-term streamflow series, many data mining techniques including the sedimentological method, the hydrological field survey method, and the documentary analysis method can be applied (Longfield et al., 2018). Nevertheless, low temporal resolution and

insufficient accuracy of these estimations can hardly meet the demands of practical and research applications.”

Comment 8*: Line 17 needs a comma before “but”*

Answer:

We are appreciating your advice and added a comma:
“With a large topographic gradient and substantial water supply of approximately 10,000 m^3s^{-1} on the average, the upper Yangtze River is rich in hydropower resources, but subjected to destructive flash floods.”

Comment 9: *Line 23 – “Could support the development...”? Is there not already hydraulic management strategies in place?*

Answer:

It can support the development and we changed “could” with “can”. Sure, there are hydraulic management strategies in place, but they will be also developed in future. “As changes in streamflow at the Cuntan station directly influence inflow to the Three Gorges Reservoir, establishing long-term discharge series at the Cuntan station can support effective management of hydraulic projects. Besides, the longer discharge series can also provide a possibility to explore impacts of anthropogenic climate change on hydrology for international climate change research community. Therefore, we simulated daily discharge at the Cuntan hydrological station in the upper Yangtze River in the period 1861 - 2299 using available climate model outputs.”

2. Study area

Comment 10*: Is the temperate trend linked to the East Asian monsoon and topography?*

Answer:

As far as we know, spatial and temporal patterns of temperate are linked to the East Asian monsoon and topography. In order to make it clearer, we rewrote the description in revised manuscript as following:
“The upper Yangtze River have complex geomorphic types and broken topography. Mountains and plateaus account for most of the region, hills and plains are few. Influenced by the East Asia subtropical monsoon and a complex topography, climate varies across the basin with annual air temperature and precipitation being high in the southeast but low in the northwest headstream region. According to observational data, the areal averaged annual mean temperature and precipitation are 12.3 °C and 1018 mm, respectively, during 1961 - 2017 in the upper Yangtze River basin.”

__Comment 11:__ Don't say the temperate trend is obviously increasing, especially without showing a graph. By reporting a slope of "approximately 0.2C/10a" you are implying a linear trend, is this the case?

Answer:

We tried to exhibit mean air temperature from the observed data, and modified the sentence as: "According to observational data, the areal averaged annual mean temperature and precipitation are 12.3 °C and 1018 mm, respectively, during 1961 - 2017 in the upper Yangtze River basin."

__Comment 12:__ Are you referring to air temperature or water temperature?

Answer:

The mentioned temperature is air temperature. We added "air" before temperature in the revised paper (page 3, line 5):
"Influenced by the East Asia subtropical monsoon and a complex topography, climate varies across the basin with annual air temperature and precipitation being high in the southeast but low in the northwest headstream region."

__Comment 13:__ Did precipitation decrease linearly (as implied by the slope)? Does this correlate with the wet period and dry periods previously mentioned?

Answer:

It exhibited mean air precipitation from the observation, and no correlation with the wet and dry periods previously mentioned. We tried to deliver some general meteorological information about the upper Yangtze River.

3. Data and Methods

__Comment 14:__ I will let another reviewer determine whether the models were used appropriately. What do you mean the daily discharge data "were derived"?

Answer:

We revise the sentence as:
"The daily discharge record at the Cuntan station in the upper Yangtze River is available for 1970 - 1999 from the China Hydrological Yearbook - Yangtze. The rest of daily record for periods 1939 - 1969 and 2000 - 2012 is collected from the Changjiang Water Resources Commission, Ministry of Water Resources in China."

Comment 15: *Why was data from 1939-1969 not used for calibration and validation of the four hydrological models?*

Answer:

The discharge in the upper Yangtze have been observed since 1939, but majority of meteorological stations started to operate at early 1950s. The period 1979 - 1990, which included years with both wet and dry spells, was chosen as the calibration period. Then, the models were validated in two periods without changing the parameters set in the calibration: the wet spell, 1967 - 1978, and the dry spell, 1991 - 2002, following recommendation for model evaluation in reference (Krysanova et al., 2018).

Comment 16: *Reorder the first sentence of paragraph 2 on page 4.*

Answer:

We have reordered the first sentence of paragraph 2 on page 4:
"The Yangtze River is prone to be flooded because of large inter- and inner-annual variations of precipitation."

Comment 17: *Remove language from the next sentence than the disastrous floods should be mentioned.*

Answer:

We are appreciating your advice and added some reference:
"The most severe flood that can be tracked in the upper Yangtze River occured in 1870, with a flood peak of approximately 100,500 m^3s^{-1} at the Yichang station located downstream of the Cuntan station (Changjiang Water Resources Commission, 2002). The peak flows reached 63,600 m^3s^{-1} and 64,600 m^3s^{-1}, respectively, at the Cuntan station and the Yichang station during the 1931 flood, and 52,200 m^3s^{-1} and 66,800 m^3s^{-1}, respectively, during the 1954 flood (Hu and Luo, 1992; Luo and Le, 1996). During the strongest flood of the 20th century in the Yangtze River, the peak flow at the Cuntan station reached 68,500 m^3s^{-1} in 1998 (Changjiang Water Resources Commission, 2002)."

Comment 18: *How do you know that the 1870 flood was the most severe since 1153? What do you mean by "severe"?*

Answer:

The 1870 flood was recognized as the most disastrous flood events by Changjiang Water Resources Commission according to various historical records. We cited it in the revised paper as "The most severe flood that can be tracked in the upper Yangtze River occurred in 1870, with a flood peak of approximately 100,500 m^3s^{-1} at the Yichang station located downstream of the Cuntan station (Changjiang Water Resources Commission, 2002)." The "severe" is used here because the flood of 1870 reached the highest flood level in hundreds of years in the upper Yangtze river (Changjiang

Water Resources Commission, 2002).

Comment 19: *The language in this paragraph could be cleaned up and made much tighter.*

Answer:

We added references to make this paragraph much tighter: "For evaluating daily hydrograph simulation, ratio of the root mean square error to the standard deviation of measured data (RSR) is recommended (Moriasi et al., 2007). In addition, the Kling-Gupta efficiency (KGE) was developed to provide diagnostic insights into the model performance by decomposing the NSE into three components: correlation, bias and variability (Gupta et al., 2009)." We have modified statement throughout the article to make much tighter.

4.1 Climate change in the upper Yangtze basin

Comment 20: *Reorder the first sentence*

Answer:

Thanks for your suggestion. We have reordered the first sentence:
"According to ensemble mean of four GCMs, annual mean temperature in the upper Yangtze River basin in the period 1986 - 2005 was 0.49 °C higher than that in the period 1861 - 1900, the increase is lower than the global average of 0.61 °C in the same period."

4.2 Calibration and validation of the hydrological models

Comment 21: *1986/1987 does not look like a turning point to me (4.2)*

Answer:

As you mentioned, 1986/1987 does not look like a turning point. We have taken the Pettitt test and found that the turning point is in 1989. However, 1986 had comparatively less precipitation and low runoff (Fig. 5) and can be regarded as the start year of being drier. We accept your comment and rewrote the sentence and added one reference:
"Previous study found that 1986/1987 was a change-point in the observational period for south China, with more obvious increase of temperature and decrease of precipitation since then (Thomas et al., 2012)."

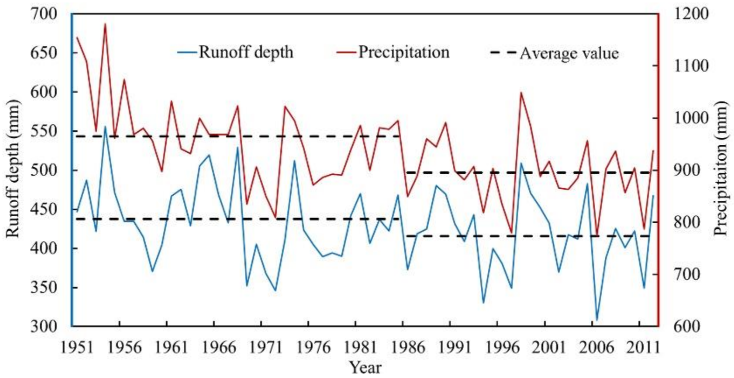

Figure 5 Annual precipitation and runoff depth observed in the upper Yangtze River basin in the period 1951 - 2012

4.3 Simulation of daily discharge from 1861 - 2299

Comment 22: *Why does the IPSL model only project a rapid decline (should be decrease?) in discharge. Seems like that would be an interesting point to discuss.*

Answer:

Yes, it is. The IPSL model has an obvious decrease in precipitation (Fig. 4b: RCP8.5), which was used by hydrological models as an input to simulate the discharge. Therefore, a significant decrease in discharge was projected. The reasons why IPSL model projected such a decrease in precipitation are not known for us.

Comment 23: *Is mean annual discharge really the best way to characterize the discharge with how much it fluctuates throughout the year?*

Answer:

One of the optimal methods to evaluate the simulated long-term discharge is to apply the mean value. We added average monthly streamflow to characterize its inter-annual fluctuation, and found a single peak pattern throughout the year (see Fig. 10a-b as follow).

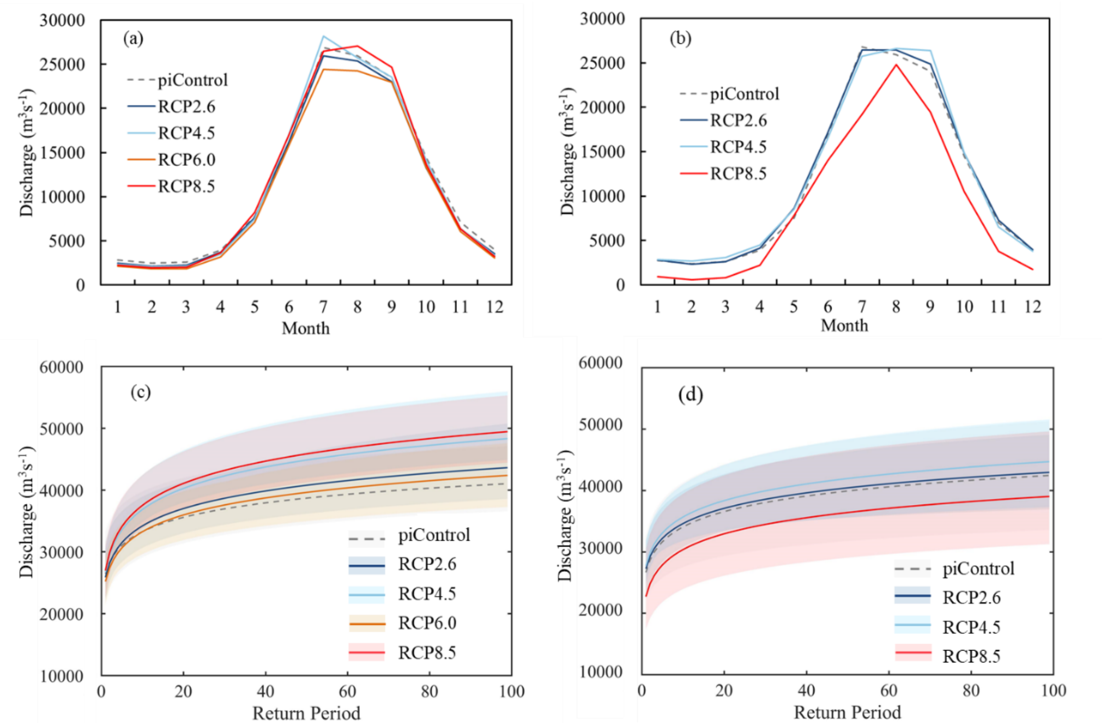

Figure 10 Comparison of monthly mean simulated discharge and return periods of daily maximum discharge at the Cuntan station for 2070 - 2099 (a, c) and 2270 - 2299 (b, d) under RCPs and the piControl scenario

> ***Comment 24:*** *Will you later go into why discharge is projected to decrease? This seems like an interesting conclusion to investigate further.*

Answer:

According to our simulation results, the daily simulated discharge will reduce with the decrease of precipitation in the future. It is a good idea to further study the reasons why discharge is projected to decrease, which should be taken into consideration in the future.

4.4 Data availability

> ***Comment 25:*** *What do you mean 16 sequences of daily discharge?*

Answer:

4 GCMs and 4 different hydrological models are used to simulate river discharge in our study, and each GCM was inputted into 4 hydrological models. Therefore, total of 16 discharge series are outputted.

5 Summary and conclusions

> ***Comment 26:*** *I would like to see discussion and conclusions separated unless this is the journal's recommended style.*

Answer:

There is no specific recommend style in ESSD. Section 5 is a summary about how we obtained this dataset and verified its reliability. Thus, we changed the subtitle "Conclusions and discussion" to "Summary and conclusions".

> ***Comment 27:*** *Is there no updated land use map since 1990? I would think the effects of human induced change could completely change the results and needs to be incorporated. There has been tremendous growth in the last (almost) 30 years in China.*

Answer:

Actually, influence of human management has aggravated and the land cover changed quite obviously in the last 30 years in China. Therefore, calibration is conducted in a comparatively earlier period of 1979-1990. In order to compare the trend of daily simulated discharge under a changing climatic background and keep the hydrological model stable with high performance in different period, we used the 1990 land use as single geographical data to simulate the daily discharge by controlling the variable as little as possible.

> ***Comment 28:*** *Figure 3a could be a dynamic figure. Can you make it clearer? If it's not possible in one graph, maybe split it up? Figure 3 captions needs more information.*

Answer:

Fig. 4a and 4b (previous Fig. 3) show the annual dynamics of precipitation for a long period, splitting it into subperiods might not be reasonable.

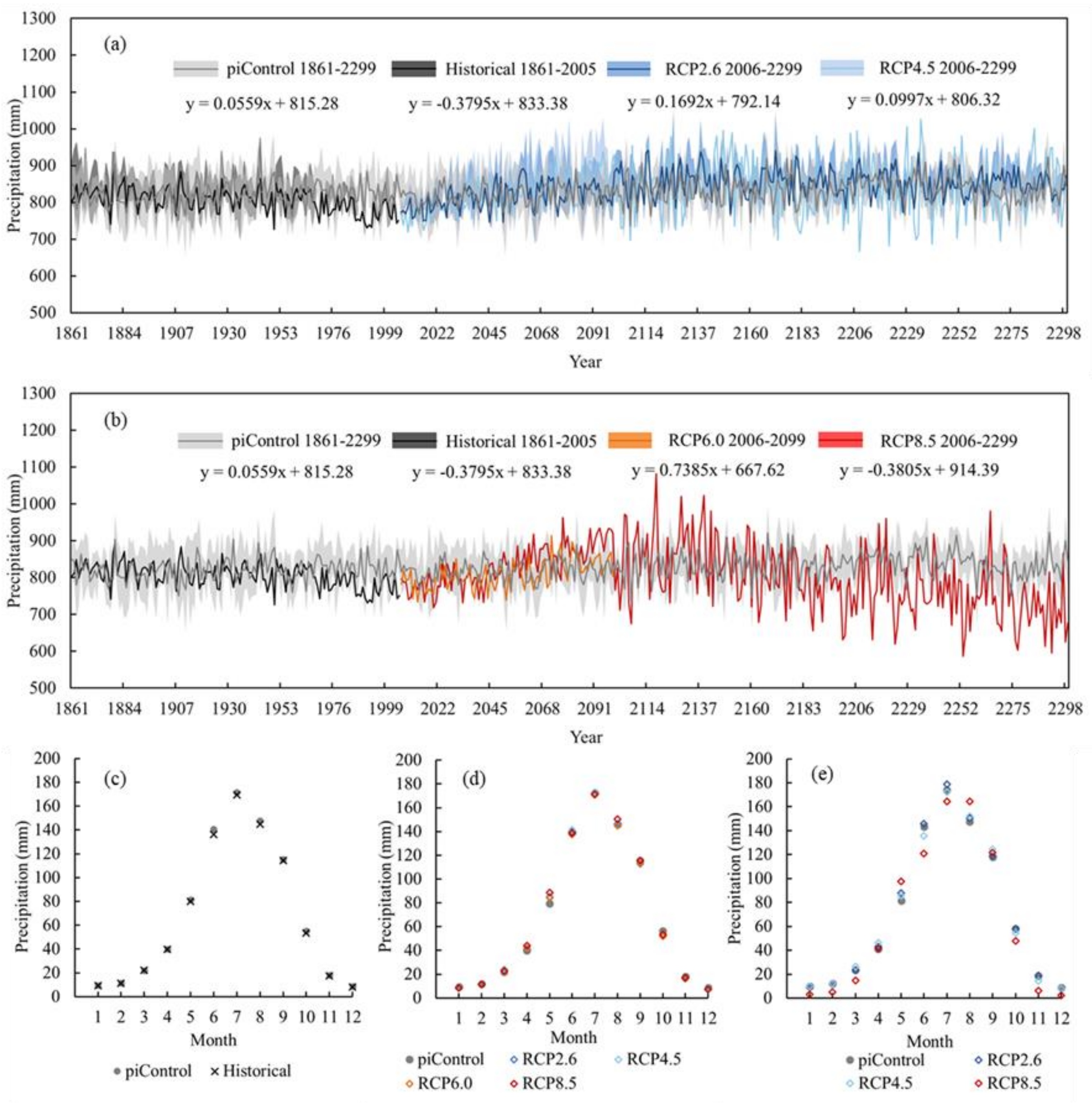

Figure 4 Annual (a-b) and long-term average monthly (c-e) dynamics of precipitation in the upper Yangtze basin: comparison of the piControl scenario with the historical and anthropogenic climate change RCP scenarios (periods: a: 1861 - 2299; b: 1861 - 2299; c: 1861 - 2005; d: 2006 - 2099; and e: 2100 - 2299)

Comment 29: *Figure 4 – why the two different average value lines? Needs to be discussed in the figure caption. Is this the wet/dry periods?*

Answer:

Fig. 5 illustrates the wet/dry periods based on the observed discharge and meteorological data. Two dotted straight lines represent the mean discharge and precipitation, respectively, in the wet and dry period.

Comment 30: Figure 5 – include r values

Answer:

We have redrawn Fig. 5 (now Fig. 6), which compares the simulated and observed Q10, Q90 discharges at the Cuntan station in the calibration and validation periods.

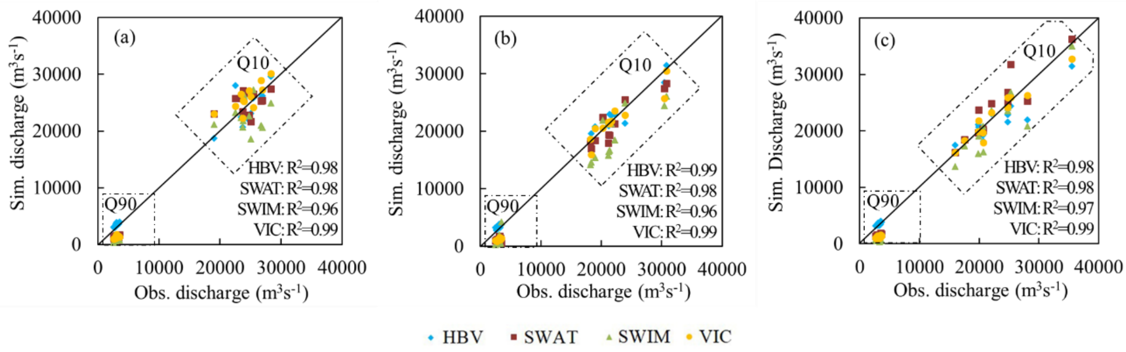

Figure 6 Comparison of the simulated and observed Q10, Q90 percentiles at the Cuntan station in the calibration period 1979 - 1990 (a) and validation period 1967 - 1978 and 1991 - 2002 (b-c)

Comment 31: *Figure 8 – Does historical data only go to 2005? This needs to be mentioned earlier in the paper. Is there more data available ie through at least 2018 or whenever the analysis was started?*

Answer:

The fourth paragraph in introduction describes the time ranges of GCMs' historical period as defined in the ISIMIP protocol (Frieler et al., 2017). It was defined that historical anthropogenic climate change period is 1861-2005, which can be compared with piControl scenario without human-induced influences and future RCPs, and we followed the suggestions in the protocol.

Best regards,

Chao Gao and co-authors

A 439-year simulated daily discharge dataset (1861-2299) for the upper Yangtze River, China

Chao Gao[1], Buda Su[2], Valentina Krysanova[3], Qianyu Zha[1], Cai Chen[1], Gang Luo[1], Xiaofan Zeng[4], Jinlong Huang[5], Min Xiong[6], Liping Zhang[7], Tong Jiang[5]

[1]Department of Geography & Spatial Information Techniques, Ningbo University, Ningbo, 315211, China;

[2]National Climate Centre, China Meteorological Administration, Beijing 100081, China;
[3]Potsdam Institute for Climate Impact Research, Potsdam, Germany;
[4]School of Hydropower and Information Engineering, Huazhong University of Science and Technology, Wuhan, 430074, China;
[5]Collaborative Innovation Center on Forecast and Evaluation of Meteorological Disasters, Institute for Disaster Risk Management (iDRM), School of Geographical Science, Nanjing University of Information Science & Technology, Nanjing 210044, China;
[6]Bureau of Hydrology, Changjiang River Water Resources Commission, Wuhan, 430010, China;
[7]State Key Laboratory of Water Resources and Hydropower Engineering Science, Wuhan University, Wuhan, 430072, China

Correspondence to: Tong Jiang (jiangtong@nuist.edu.cn)

Abstract. The outputs of four Global Climate Models (GFDL-ESM2M, HadGEM2-ES, IPSL-CM5A-LR and MIROC5), which were statistically downscaled and bias corrected, were used to drive four hydrological models (HBV, SWAT, SWIM and VIC) to simulate the daily discharge at the Cuntan hydrological station in the upper Yangtze River from 1861 to 2299. As the performances of hydrological models in various climate conditions could be different, the models were first calibrated in the period from 1979 to 1990. Then, the models were validated in the comparatively wet period, 1967 - 1978, and in the comparatively dry period, 1991 - 2002. A multi-objective automatic calibration programme using a univariate search technique was applied to find the optimal parameter sets for each of the four hydrological models. The Nash-Sutcliffe efficiency (NSE) of daily discharge and the weighted least squares function (WLS) of extreme discharge events, represented by high flow (Q10) and low flow (Q90), were included in the objective functions of the parameterization process. In addition, the simulated evapotranspiration results were compared with ~~evapotranspiration data from the~~ GLEAM evapotranspiration data ~~project~~ for the upper Yangtze basin. For evaluating the performances of the hydrological models, the NSE, modified Kling-Gupta efficiency (KGE), ratio of the root mean square error to the standard deviation of the measured data (RSR) and Pearson's correlation coefficient (r) were used. The four hydrological models ~~showed good performance in the calibration and validation periods~~ reach satisfactory simulation results

both in the calibration and validation periods. In this study, the daily runoff discharge was is simulated for the upper Yangtze River under the preindustrial control (piControl) scenario without anthropogenic climate change, from 1861 - 2299, and for the historical period 1861 - 2005, and for 2006 to 2299 under the RCP2.6, RCP4.5, RCP6.0 and RCP8.5 scenarios in the period from 2006 to 2299. The long-term daily discharge datasets for the upper Yangtze River provide streamflow trends in the future and clues regarding to what extent human-induced climate change could impact streamflow. can be used in the international context and water management, e.g. in the framework of Inter-Sectoral Impact Model Intercomparison Project (ISIMIP) by providing clue to what extent human-induced climate change could impact streamflow and streamflow trend in future. The datasets are available at the https://doi.org/10.4121/uuid:8658b22a-8f98-4043-9f8f-d77684d58cbc (Gao et al., 2019).

1 Introduction

With the progress of industrialization, global warming has been escalating. Global warming Global warming is the long-term rise in average temperature of the earth's climate system. Warming temperature alters global water circulation processes and could significantly influence the sustainability of the social society and economy (Jung et al., 2011). The variation in water resource availability in the context of global warming has become the focus of hydrological research is acknowledged as a focus of many international research projects (Su et al., 2015; Stagl et al., 2016; Raman et al., 2018; Maisa et al., 2019). The long-term accurate (as much as possible) daily runoff sequences discharge time series are crucial for an in-depth understanding of the changes in global water resources in streamflow, and they are needed for subsequent research climate change impact studies. However, runoff is commonly monitored for only discharge is monitored usually only for short observational periods in most river basins.

To date, the sedimentological method, hydrological field survey method, and recorded historical documents have been used to develop long-term runoff series. For generation of the long-term streamflow series, many data mining techniques including the sedimentological method, the hydrological field survey method, and the documentary analysis method can be applied (Longfield et al., 2018). However Nevertheless, the low temporal resolution and insufficient estimation accuracy of these methods and resources estimations can hardly meet the demands of practical and research applications. Instead, the observed climatic variables and the outputs of Global Climate Models (GCMs) and Regional Climate

Models (RCMs) climate models have often been used to drive hydrological models to evaluate changes in runoff streamflow in the context of climate change (Braud et al., 2010; Chen et al., 2017; Su et al., 2017; Dahl, 2018; Seneviratne et al., 2018). However But there is a lack of research on the quantitative estimation of long-term runoff streamflow for periods longer than 400 years, especially under scenarios with and without anthropogenic climate change (Meaurio, 2017).

The Yangtze River is the longest river in China. It originates on from the Tibetan Plateau and enters the East China Sea after flowing through 11 provinces. With a large topographic gradient and substantial mean annual water supply of approximately 10,000 m^3s^{-1} on the average, the upper Yangtze River is rich in hydropower resources, but is subjected to destructive flash floods. The Yangtze River basin has the longest hydrological observations in China. with Data provided by the Cuntan hydrological station, which started operating in 1939, This data availability facilitates hydro-meteorological studies in the instrumental period (Su et al., 2008; Wang et al., 2008; Su et al., 2017). As changes in runoff streamflow at the Cuntan station directly influence the water supply of inflow to the Three Gorges Reservoir, establishing a long-term runoff discharge time series at the Cuntan station could can support the development of hydraulic management strategies in the upper Yangtze River. effective management of hydraulic projects. Besides, the longer discharge series can also provide a possibility to explore impacts of anthropogenic climate change on hydrology for international climate change research community. Therefore, the main aim of this study was to we simulated daily discharge at the Cuntan hydrological station in the upper Yangtze River in the period from in the period 1861 - 2299 using available climate model outputs. The outputs of four downscaled GCMs (GFDL-ESM2M, HadGEM2-ES, IPSL-CM5A-LR, and MIROC5) are utilized to drive and four hydrological models (HBV, SWAT, SWIM and VIC) were utilized to simulate runoff discharge at the Cuntan station. The climate forcing comprised (a) the scenarios with anthropogenic climate change for the period 1861 - 2299, which was is subdivided into the historical period (1861 - 2005) and the future period (2006 - 2299) under different Representative Concentration Pathway (RCP) scenarios, and (b) the preindustrial control (piControl) scenario without human-induced climate change for the period 1861 - 2299, which was is used as a reference to detect the influence of anthropogenic climate change on discharge streamflow in the upper Yangtze River.

2 Study Area

~~With a catchment area of approximately 860,000 km^2, the mean annual runoff at the Cuntan hydrological station (29 ° 37 ′ N, 106 ° 36 ′ E) in the upper Yangtze River is 352.7 billion m^3, and the maximum peak discharge is 73,800 m^{3}s^{-1} (in 1945) for the period of instrumental measurements beginning in 1939. Influenced by the East Asian subtropical monsoon and a complex topography, the annual mean temperature exhibited an obvious increasing trend in the upper Yangtze from 11.4 °C (1950s) to 12.4 °C (2010s), with a slope of approximately 0.2 °C / 10 a. The annual precipitation decreased from 900 mm (1950s) to 845 mm (2010s), with a slope of -11 mm / 10 a.~~

The catchment area of the Cuntan hydrological station (29 ° 37 ′ N, 106 ° 36 ′ E) in the upper Yangtze River is approximately 860,000 km2, and 352.7 billion m3 water is flowing through this point annually with average discharge of 109,34 m3s-1 in the period of instrumental measurements beginning in 1939. Location of the Cuntan hydrological station, 311 GCM grids, meteorological stations and spatial distribution of the land use and soil types in the upper Yangtze River basin are shown in Fig. 1. Prairie grassland and acid purple soil are the most widespread of land use and soil type in the upper Yangtze River basin. The upper Yangtze River have complex geomorphic types and broken topography. Mountains and plateaus account for most of the region, hills and plains are few. Influenced by the East Asia subtropical monsoon and a complex topography, climate varies across the basin with annual air temperature and precipitation being high in the southeast but low in the northwest headstream region. According to observational data, the areal averaged annual mean temperature and precipitation are 12.3 °C and 1018 mm, respectively, during 1961 - 2017 in the upper Yangtze River basin.

3 Data and Methods

3.1 Climate scenarios

The outputs of the GCMs (GFDL-ESM2M, HadGEM2-ES, IPSL-CM5A-LR, and MIROC5) were statistically downscaled and bias corrected on a regular 0.5 × 0.5 ° resolution grid using a first-order conservative remapping scheme (Frieler et al., 2017; Lange, 2018). The GFDL model was developed by the Geophysical Fluid Dynamics Laboratory, Princeton University, USA, and all its integrations (approximately 100 in total), including GFDL-ESM2M and GFDL-ESM2G, were completed for the Coupled Model Intercomparison Project Phase 5 (CMIP5) protocol (Taylor et al., 2012). HadGEM2-ES is a coupled earth system model that was developed by the Met Office Hadley Centre, UK, for the CMIP5 centennial simulations (Jones et al., 2011). The IPSL-CM5A-LR model was developed by the Institute Pierre

Simon Laplace, France, and the model was built around a physical core that includes atmosphere, land surface, ocean and sea ice components (Dufresne et al., 2013). MIROC5 is a new version of the atmosphere-ocean GCM that was developed by the Japanese research community (Watanabe et al., 2010).

~~Due to a~~ Lack of long-term homogeneous observational data and existing of ~~the~~ confounding influence ~~of~~ from socioeconomic drivers, make GCM simulations rarely cover the preindustrial period. In this study, ~~the simulated~~ climate ~~conditions~~ simulations include a piControl scenario, representing ~~a preindustrial climate with a~~ a climate with natural variability under stable CO_2 concentration of 286 ppm, a historical scenario, representing the historical CO_2 concentration, and future RCP scenarios, representing various future CO_2 concentration pathways. The availability of climate scenarios for the different periods is shown in Table 1 (see also Frieler et al., 2017). Note that not all simulations ~~are available after 2099: from three models for RCP2.6, only from IPSL for RCP4.5 and RCP8.5, and no simulations for RCP6.0~~ cover 22nd and 23rd century. Data after 2099 are available from three models under RCP2.6, only from IPSL under RCP4.5 and RCP8.5, but no simulations under RCP6.0.

3.2 Observed meteorological and hydrological data

The observed daily meteorological data from 1951 - 2017 from 189 ground-based stations in the upper Yangtze River used in this study were quality controlled by considering changes in instrument type, station relocations, and trace biases at the National Meteorological Information Center of the China Meteorological Administration (Ren et al., 2010), which was inputted into the hydrological models by spatial interpolation. During 1951 - 2017, annual precipitation shows a decreasing trend, with multi-year average of 935 mm, and annual mean temperature has shown a positive trend with multi-year average of 10.5 °C. ~~The daily discharge data for the period 1939 - 2012 at the Cuntan station in the upper Yangtze River were derived from the China Hydrological Year book - Yangtze. Data from 1967 - 2002 were used for calibration and validation of the four hydrological models.~~ The daily discharge record at the Cuntan station in the upper Yangtze River is available for 1970 - 1999 from the China Hydrological Yearbook - Yangtze. The rest of daily record for periods 1939 - 1969 and 2000 - 2012 is collected from the Changjiang Water Resources Commission, Ministry of Water Resources in China.

~~With large variations in seasonal and interannual precipitation, the Yangtze River is prone to flooding. Disastrous flood events that occurred in 1870, 1931, 1954 and 1998 should be mentioned. In 1870, the most severe flood since 1153 occurred in the upper Yangtze River, with a flood peak at the Yichang~~

station (downstream of the Cuntan station) of approximately 100,500 m^3s^{-1}. The peak flows at the Cuntan and Yichang stations reached 63,600 m^3s^{-1} and 64,600 m^3s^{-1}, respectively, during the 1931 flood event and 52,200 m^3s^{-1} and 66,800 m^3s^{-1}, respectively, during the 1954 flood event. In 1998, the strongest flood of the 20th century occurred in the Yangtze River, and the peak flow at the Cuntan station reached 68,500 m^3s^{-1}.

The Yangtze River is prone to be flooded because of large inter- and inner-annual variations of precipitation. The most severe flood that can be tracked in the upper Yangtze River occurred in 1870, with a flood peak of approximately 100,500 m3s-1 at the Yichang station located downstream of the Cuntan station (Changjiang Water Resources Commission, 2002). The peak flows reached 63,600 m3s-1 and 64,600 m3s-1, respectively, at the Cuntan station and the Yichang station during the 1931 flood, and 52,200 m3s-1 and 66,800 m3s-1, respectively, during the 1954 flood (Hu and Luo, 1992; Luo and Le, 1996). During the strongest flood of the 20th century in the Yangtze River, the peak flow at the Cuntan station reached 68,500 m3s-1 in 1998 (Changjiang Water Resources Commission, 2002).

3.3 GLEAM evapotranspiration data

In addition to river discharge data, Evapotranspiration data from the Global Land Evaporation Amsterdam Model (GLEAM) for the period 1986 - 2005 that were released by the University of Bristol (Miralles et al., 2011) were are used in our study to cross-check the performances of the hydrological models by means of the geographic information system (GIS) tools. GLEAM is comprised of four mutually connected units: the Gash interception module, soil module, stress module, and Priestley-Taylor module. The remote sensing data were assimilated to obtain monthly evapotranspiration with a spatial resolution of 0.25°. The GLEAM data was generated based on a variety of satellite-sensor products at monthly scale with a spatial resolution of 0.25°. The spatial distributions of simulated evapotranspiration with that from GLEAM are compared by GIS techniques, and kappa value of confusion matrix is also applied to evaluate the accuracy of simulated evapotranspiration (taking VIC output as an example) by refer to GLEAM.

3.4 Hydrological models and parameterization

Four hydrological models, HBV (Bergstrom et al., 1973), SWAT (Arnold et al., 1998), SWIM (Krysanova et al., 2005) and VIC (Liang et al., 1994), were used to simulate river discharge at the Cuntan hydrological station. are used to simulate river discharge at the Cuntan hydrological station, and a flowchart of the hydrological modelling process is shown in Fig. 2. A brief introduction to these four hydrological models is given in Table 2 (see also Hattermann et al., 2017).

~~3.5 Calibration and validation methods~~

~~A~~ The univariate search technique, which can evaluate the informativeness of each feature individually, ~~was~~ is used to calibrate the parameters ~~(Lai et al., 2006)~~. The objective functions include~~d~~ the Nash-Sutcliffe efficiency (NSE) of daily discharge (Nash and Sutcliffe, 1970) and the weighted least squares function (WLS) of high flow (Q10) and low flow (Q90). To achieve the maximum NSE and minimum ~~difference~~ gap between the observed and simulated ~~extremes~~, ~~the parameter values were changed more than 2,000 times within the ranges of the valid parameter scope.~~ parameterization processes are iterated over 2,000 times within the ranges of the valid parameter scopes in Table 3 (Lai et al., 2006).

For evaluating daily hydrograph simulations ~~(Moriasi et al., 2007)~~, ~~the~~ ratio of the root mean square error to the standard deviation of measured data (RSR) is recommended (Moriasi et al., 2007). In addition, the Kling-Gupta efficiency (KGE) was developed to provide diagnostic insights into the model performance by decomposing the NSE into three components: correlation, bias and variability (Gupta et al., 2009). In this study, four criteria, the NSE, RSR, Pearson's correlation coefficient (r) and KGE, ~~were~~ are applied to the daily time series to evaluate the performances of the hydrological models (~~Table 3~~ Krysanova et al., 2018; Table 4) .Thresholds of acceptance of four criteria are derived from the references (Nash and Sutcliffe, 1970; Moriasi et al., 2007; Huang et al., 2012; King et al., 2012).

.

~~3.6~~ 3.5 Geospatial information

A digital elevation model (DEM) with a resolution of 90 m from the Shuttle Radar Topography Mission database was used in this study. The soil property data were obtained from the Harmonized World Soil Database of the Food and Agriculture Organization of the United Nations (http://www.fao.org/), and the spatial distribution of soil types (1:1,000,000) ~~was~~ is taken from the Institute of Soil Science of the Chinese Academy of Sciences (CAS). A land use map (1:1,000,000) ~~for 1990 was~~ from ~~provided by~~ the Data Center for Resource and Environmental Sciences ~~of the CAS~~, ~~and this land use map was applied in the piControl, historical and RCP scenario periods (see discussion in Section 5).~~ CAS is applied for all hydrological runs under various climate conditions including the piControl, the historical and the RCP scenarios.

4 Results

4.1 Climate change in the upper Yangtze basin

~~Compared to that in the piControl scenario, the annual mean temperature in the historical period, 1861-2005, was slightly higher until the 1980s and showed a notable increase in the period 1986 - 2005 (Fig. 2) according to the ensemble mean of four GCMs. The annual mean temperature in 1986 - 2005 was 0.49 °C higher than that in the period 1861 - 1900 in the upper Yangtze basin, which was lower than the global average of 0.61 °C in the same period. Compared to the piControl scenario, under the RCP scenarios, the annual mean temperature was projected to increase significantly in the 21st century, by 1.1 - 6.9 °C. According to climate model projections, after 2100, the surface air temperature will remain stable under RCP2.6 and increase only slightly under RCP4.5, but a significant increase in temperature will continue under the RCP8.5 scenario, with an increase up to 13.5 °C compared to that in the piControl scenario (Fig. 2a).~~ According to ensemble mean of four GCMs, annual mean temperature in the upper Yangtze River basin in the period 1986 - 2005 is 0.49 °C higher than that in the period 1861 - 1900, the increase is lower than the global average of 0.61 °C in the same period. Compared to the piControl scenario, annual mean temperature is projected to increase significantly in the 21st century, by 1.85 ~ 3.31 °C under RCPs. After 2100, surface air temperature will remain stable under RCP2.6 and increase only slightly under RCP4.5, but a significant increase in temperature will continue under RCP8.5, with an increase up to 13.5 °C by 2299 compared to the piControl scenario (Fig. 3a, Table 5). The visible abruption ~~changes~~ in temperature in the year 2100 under RCP4.5 and RCP8.5 in ~~Fig. 2a~~ Fig. 3a are due to the fact that only the IPSL model runs were available after 2100 for these scenarios.

The long-term average ~~seasonal~~ monthly dynamics of temperature ~~were represented by~~ show a single-peak curve, ~~and~~ with July is the hottest month ~~was the month with the highest temperature under both the RCP scenarios and the piControl scenario~~. In the period 1861-2005, the ~~seasonal~~ inner-annual distribution pattern~~s~~ of temperature ~~were~~ is very similar for the piControl and the historical scenarios (Fig. 3b) ~~two scenarios, the piControl and historical scenarios (Fig. 2b)~~. However, differences in the monthly temperatures between the RCP scenarios and piControl scenario become apparent with time (~~Fig. 2c-d~~ Fig. 3c-d). Taking the temperature in July as an example, ~~the~~ differences between the two scenarios ~~were~~ are approximately 1.9 ~ 3.2 °C in the 21st century ~~and~~ but will enlarge to 1.7 ~ 12 °C in the period 2100 - 2299 ~~(Fig. 2c-d).~~

Compared with the precipitation in the under piControl scenario, which had has no monotonic trend, the annual precipitation in the historical scenario showed a negative trend in the upper Yangtze basin, with an obvious decrease in the period 1986 - 2005 of approximately 7 % (60 mm). Under the RCP scenarios, the annual precipitation was projected to increase in the 21st century by up to 25.4 % compared to the precipitation simulated in the piControl scenario. The increase in precipitation tends to be stable, but the variation amplifies beginning in 2100. Especially under the RCP8.5 scenario, a wide range of fluctuations was projected with a variance as high as 86.1, which is 60.5 % higher than that in the piControl scenario (Fig. 3a). annual precipitation is approximately 2 % (16 mm) less in 1861 - 2005 under historical scenario. With relative to the piControl scenario, changes of annual precipitation will be -1.2% ~ 1.3 % in the 21st century under RCPs, and will be 0.6 %~ 2.2 % in the 2100 - 2299 under RCP 2.6 and 4.5. Under RCP8.5, relative change of annual precipitation is -5.7 % and a wide range of fluctuations is projected with a variance as high as 94.3 in 2100 - 2299, which is 63.2 % higher than the piControl scenario (Fig. 4a-b, Table 5).

The long-term average seasonal monthly precipitation was represented by shows a single-peak curve, with the precipitation highest in July and the lowest precipitation in December and January. The differences in the long-term average seasonal monthly precipitation under the RCPs scenarios and the piControl scenario were are projected to be grow from -1.9 ~ 1.3 % before 2100 but would grow to -5.4 - 2.2 % in the period 2100 - 2299 (Fig. 3b-d Fig. 4c-e).

4.2 Calibration and validation of the hydrological models

Previous study found that 1986/1987 was a change-point in the observational period for south China, with more obvious increase of temperature and decrease of precipitation since then (Thomas et al., 2012). Fig. 4 Fig. 5 shows the that observed annual precipitation and runoff observed depth in the upper Yangtze basin in the period 1951 - 1986 are 1951 - 2012. The mean observed precipitation and runoff depth were approximately 965 mm and 437 mm, respectively, in the period 1951 - 1986 and decreased by 7 % and 5 % to 895 mm and 415 mm, respectively, in the period 1987 - 2012. As shown in Fig. 4, 1986/1987 could be considered a turning point; the climate conditions become drier after 1987. Therefore, the period 1979 - 1990, which included years with both comparatively wet and dry spells, was is chosen as the calibration period. Then Subsequently, the hydrological models were are validated in two periods without changing the parameters found set during the calibration: the wet spell, 1967 - 1978, and the dry spell, 1991 - 2002.

Based on the NSE, RSR and r values, all four hydrological models performed quite well in both the calibration and validation periods for the simulations of daily discharge at the Cuntan station. In particular, the NSE values of all models exceeded 0.75 in the calibration period and 0.7 in the validation periods (~~Table 4~~ Table 6). The KGE values ~~were~~ are above the threshold in the calibration period for all models~~,~~ but~~ the values were~~ slightly lower in the validation period for the SWIM and VIC models.The four hydrological models ~~could~~ can also properly simulate the high flow~~s~~ represented by Q10 ~~(Fig. 5)~~ and Q90 in calibration and validation periods. ~~In addition, several of the severe observed floods that were mentioned previously were reproduced quite well by the simulated data, namely: extreme flood event of approximately 36,000 m^3s^{-1} (Fig. 5c) occurred in 1998 during the dry period, and extreme flood event of approximately 32,000 m^3s^{-1} (Fig. 5b) occurred in 1974 during the wet period.~~ For example, Q10 result illustrates that the several severe floods mentioned previously are reproduced quite well by the model simulations: the peak flows of simulated discharge ~~in the 1930s, 1950s and 1990s~~ were 64,300 m^3s^{-1}, 53,900 m^3s^{-1} and 60,700 m^3s^{-1}, respectively, in the 1930s, 1950s and 1990s, deviating by less than 10 % from the recorded peaks (Fig. 6).

To further validate the hydrological models, ~~the~~ discharge simulated in another thirty-year historical period (1939 - 1968) ~~was~~ is compared with the observed data ~~on the monthly scale~~ (~~Fig. 6~~ Fig. 7). It is ~~visible~~ found that there are systematic underestimations of streamflow by SWAT, SWIM and VIC ~~underestimate low flow, and high flow was underestimated in some of the wet years by all hydrological models.~~ But, all four hydrological models ~~could~~ can reproduce the monthly dynamics of river flow quite satisfactorily, with NSE values of 0.79 ~ 0.84 and *r* values of 0.91 ~ 0.92.

In addition, ~~the~~ evapotranspiration outputs of ~~the four hydrological models were~~ HBV, SWAT, SWIM, VIC are compared with the GLEAM evapotranspiration data ~~output~~ (see Section 3.3) in the period 1986 - 2005. The long-term average annual evapotranspiration simulated by the four hydrological models for the upper Yangtze basin ~~was~~ is ~~477 mm (range: 426 - 523 mm), which is consistent with the results from GLEAM (466 mm)~~ 442 mm, 487 mm, 484 mm, 466 mm, respectively, quite close to the result from GLEAM (452 mm). The spatial patterns of the gridded evapotranspiration outputs of the HBV, SWAT, SWIM, VIC model and GLEAM ~~are similar~~ all show low values in the northwest but high values in the southeast of the upper Yangtze River basin (~~Fig. 7~~ Fig. 8). ~~both models show low values in the north-~~

western region but high values in the south-eastern region of the upper Yangtze basin. For the other three models, which have spatial disaggregation into sub-basins and not in grid cells, the comparison of spatial patterns of evapotranspiration with the GLEAM output is not shown. Furthermore, a matrix consisting of 500 randomly selected pixels from simulated evapotranspiration by VIC and corresponding GLEAM grids is set up to get the kappa value. The deduced kappa value of 0.62 indicates a substantial agreement of two date sources.

4.3 Simulation of daily discharge from 1861 - 2299

The simulated discharge time series for 1861 - 2299 under the piControl without anthropogenic climate change and scenarios with anthropogenic climate change effects are shown in Fig. 9a-b. scenario and scenarios with anthropogenic climate change effects are plotted for the whole period 1861 – 2299 in Fig. 8a-b. In the period 1861 – 2005, the annual mean discharge at the Cuntan station had a slightly decreasing trend, which is similar to the precipitation trend (Fig. 3), which became visible in the late 20th century. Similar to precipitation trend, annual mean discharge at the Cuntan station shows no significant trend from 1861 to 2299 under the piControl scenario. In historical period, annual mean discharge has shown a slight decrease trend in 1861 - 2005. Under the RCPs scenarios, the annual mean discharge will be in a significant upward trend in the upper Yangtze River shows a significant positive trend until 2100, with increasing variation by the end of the 21st century with increasing variation in the upper Yangtze River. Beginning in 2100, the annual mean discharge has shows no significant changes since 2100 under RCP2.6 and RCP4.5, but a rapid decline in discharge is projected under the RCP8.5 scenario in future (driven by the IPCL model only Fig. 9a-b, Table 5).

Comparison of relative changes in mean annual discharge for 2006-2099 and 2100-2299 under RCPs with that of the piControl scenario is presented in Table 7. Relative to the piControl scenario, change of annual mean discharge will be -5.1 %, -7.0 %, -10.9 % and -6.8 % respectively, under RCP2.6, RCP4.5, RCP6.0 and RCP8.5, in 2006 - 2099. And the relative change of annual mean discharge will be 1.4 %, 1.1 % and -13.8 %, respectively, under RCP2.6, RCP4.5 and RCP8.5 in 2100 - 2299 (Table 7).

Under RCP2.6, RCP4.5 and RCP6.0, Q10 and Q90 discharge will be lower than that under the piControl scenario in 2006 - 2099. The relative changes of Q10 will be 1.4% higher but that of Q90 will be -12.6% lower under RCP8.5 than that under the piControl scenario in 2006 - 2099.

In 2100 - 2299, a higher Q10 discharge is projected under RCP2.6 and RCP4.5 than the piControl scenario. Meanwhile, a higher Q90 discharge under RCP2.6 but a lower Q90 discharge under RCP4.5 is projected. But the relative changes of Q10 and Q90 discharge will reach - 5.5 % and - 34.2 % due to the rapid declining of discharge under RCP8.5 in 2100 - 2299. The results indicate there will be more extreme hydrological events in the long run, especially under RCP8.5.

Similar to precipitation and temperature, average monthly discharge in 2070 - 2099 and 2270 - 2299 under both the piControl and RCP scenarios show single peak. Under RCP 4.5, a higher flood volume of August is projected in periods of 2070 - 2099 and 2270 - 2299 than the piControl scenario. Meanwhile, a higher volume in 2070 - 2099 but a lower in 2270 - 2299 under RCP8.5 is projected. Under RCP2.6, the flood volume of August is similar to piControl in both periods (Fig. 10a-b). The Generalized Logistic Distribution (GLD), which is the optimistic distribution by Kolmogorov - Smirnov goodness of fit test, is applied to describe the statistical distribution of the daily maximum discharge (represented by annual Q10) for 2070-2099 and 2270-2299. It is found that the return level of daily maximum discharge under RCP2.6, RCP4.5, RCP6.0 and RCP8.5 are higher than piControl scenario in 2070 - 2099 (Fig. 10c). Under RCP 4.5, a higher average of return level of daily maximum discharge is projected in periods of 2070 - 2099 and 2270 - 2299 than the piControl scenario. For RCP8.5, the average of return level of daily maximum discharge is higher in 2070 - 2099 but lower in 2270 - 2299 than piControl scenario. Under RCP2.6, the average of return level of daily maximum discharge is similar to piControl scenario in both periods (Fig. 10c-d).

Higher return levels of daily maximum discharge were projected in the period 2070 – 2099 compared to those in the period 2170 – 2199 (Fig. 8c-d). Generally, the higher the emission scenario, the larger the return level is, with the exception of RCP6.0. When the model projections are taken as a whole, high discharge in the upper Yangtze River shows an increasing trend in the 21st century, turning into a decreasing trend in the 22nd century.

We also compared the changes under the climate warming scenarios in the whole future period 2006 – 2299 to those in the piControl scenario. According to the simulation results of the four hydrological models, the mean annual discharge in the piControl scenario is 11,517 m^3s^{-1}. Relative to that in the piControl scenario, the mean discharge is projected to decrease by 1.7-13.3 % under the RCP scenarios in the period 2006 – 2299 (see Table 5). This result indicates that anthropogenic climate change will induce a decrease in discharge in the upper Yangtze River, and the decrease would be larger under the higher RCP scenarios.

Regarding extremes, the Q90 discharge was projected to be lower under all RCP scenarios compared to that in the piControl scenario. Additionally, the Q10 discharge would also be slightly lower under the three RCP scenarios (except for RCP4.5) in the period 2006 – 2099 (Table 5), indicating an alleviation of flood risks but an aggravation of droughts in the future under global warming.

Regarding discharge variation, both the standard deviation and the coefficient of variation are higher under the RCP scenarios than under the piControl scenario (Table 5), which means that the discharge

~~variation range would increase with the intensification of human-induced climate change.~~

4.4 Data availability

The current study ~~produced~~ generates ~~the~~ daily discharge time series for the upper Yangtze River at the ~~(~~Cuntan ~~gauge~~ gauging station~~)~~ in the period 1861 - 2299 under scenarios with and without anthropogenic climate change. The river discharge ~~was~~ is simulated by four hydrological models, HBV, SWAT, SWIM, and VIC driven by four downscaled and bias-corrected GCMs (GFDL-ESM2M, HadGEM2-ES, IPSL-CM5A-LR and MIROC5), and the datasets are available at https://doi.org/10.4121/uuid:8658b22a-8f98-4043-9f8f-d77684d58cbc (Gao et al., 2019).

(1) Scenario without anthropogenic climate change (piControl):

A total of 16 sequences of daily discharge at the Cuntan hydrological station in the upper Yangtze River are ~~the~~ outputs of the four hydrological models that ~~were~~ are driven by the four GCMs in the period 1861 - 2299.

(2) Scenarios with anthropogenic climate change:

Historical period: A total of 16 sequences of daily discharge at the Cuntan station in the upper Yangtze River are ~~the~~ outputs of the four hydrological models that ~~were~~ are driven by the four GCMs in the period 1861 - 2005.

RCP2.6 scenario: a total of 16 sequences of daily runoff at the Cuntan station in the upper Yangtze River are the outputs of the four hydrological models that were driven by the four GCMs in the period 2006 - 2299 (for GFDL-ESM2M, the sequences are for the period 2006 - 2099).

RCP4.5 scenario: a total of 16 sequences of daily discharge at the Cuntan station in the upper Yangtze River are ~~the~~ outputs of the four hydrological models that ~~were~~ are driven by the four GCMs in the period 2006 - 2099 (for IPSL-CM5A-LR, the sequences are for the period 2006 - 2299).

RCP6.0 scenario: a total of 16 sequences of daily discharge at the Cuntan station in the upper Yangtze River are ~~the~~ outputs of the four hydrological models that ~~were~~ are driven by the four GCMs in the period 2006 - 2099.

RCP8.5 scenario: a total of 16 sequences of daily discharge at the Cuntan station in the upper Yangtze River are ~~the~~ outputs of the four hydrological models that ~~were~~ are driven by the four GCMs in the period 2006 - 2099 (for IPSL-CM5A-LR, the sequences are for the period 2006 - 2299).

5 Conclusions and Discussion Summary and conclusions

Using four GCMs (GFDL-ESM2M, HadGEM2-ES, IPSL-CM5A-LR and MIROC5), changes in temperature and precipitation in the upper Yangtze River basin were are analysed from 1861 to the end of 23th century under conditions with anthropogenic climate change (the four RCP scenarios) and for a scenario without human-induced anthropogenic climate change (abbreviated as the piControl scenario), and the scenarios were compared. The discharge at the Cuntan station in the period 1861 - 2299 was is simulated by four hydrological models (HBV, SWAT, SWIM and VIC) that were driven by the four GCMs, and changes in discharge in a warming world were are compared with those in the piControl scenario.

To ensure the reliability of the simulated runoff data, a multi-objective automatic calibration programme using a univariate search technique was is applied to obtain the optimal parameter sets for each hydrological model. For the objective functions, the daily discharge and indicators of high and low flows were are considered. For the calibration, Four criteria, including the NSE, KGE, RSR and r, were are used to evaluate the simulation abilities of the hydrological models parameterization results. To ensure assess the models' ability to satisfactorily represent simulate discharge under different climate conditions, the hydrological models were are additionally validated both in dry and wet periods. In addition Besides, a cross-validation method was applied by comparing the evapotranspiration outputs simulated by the hydrological models with the remote-sensing-based evapotranspiration dataset from the GLEAM. evapotranspiration outputs by simulation process are compared with remote-sensing-based evapotranspiration from the GLEAM dataset to further validate performance of the models.

The results showed that the four hydrological models had good performance in the calibration period and in the both dry and wet periods. Previous studies have also shown that the HBV, SWAT and VIC hydrological models could be applied to the Cuntan station in the upper Yangtze River after calibration (Huang et al., 2016；Su et al., 2017; Chen et al., 2017). Our study proves that HBV, SWAT, SWIM and VIC models can satisfactorily simulate precipitation-runoff relation in a changing climate. Moreover, the simulated extreme peak values in the 1930s, 1950s and 1990s were are also in good agreement with the historical documented records of the catastrophic floods in the Yangtze River.

Although the simulation results were are tested and validated with by several criteria, there are still uncertainties that could influence the outputs. These uncertainties are associated with the input GIS data (e.g., land use data), downscaling selection of the GCMs, and setting the climatic scenarios, the model calibration procedure, and exclusion of water management practices, etc (Gerhard, et al., 2018). First, as no dynamic land use data were are available for the historical period before the 1980s and for the future, a static land use for 1990 was is used for simulating river discharge before (including the piControl period) and after the industrial revolution (historical and RCP scenarios). Second, though although the most up-to-date climate scenarios were are used in this study, downscaling of the GCMs and setting the climate scenarios still contributed to the uncertainty in the hydrological simulation results. Third, the hydrological models were parameterized using the automatic calibration programme. The parameter effects and model applicability were are assessed according to the NSE, KGE, and RSR criteria. However, due to equifinality, there could be other parameter sets that would may result in a similarly good model performance. Actually, the Combination of parameters and not the choice of individual parameters ultimately influences the result (Cheng et al., 2014). There is a lack of analyses on the effects of different parameter combinations in this study, and the uncertainty related to specific parameters in the models needs to be analysed further. Fourth, since the 1990s, human interferences have escalated in the upper Yangtze River. The construction of dikes and reservoirs may alter the timing and volume of peak discharge and low base flow. Without consideration of The effects of human interferences, but rather focus merely on the natural streamflow is one of the limitations in this study were not considered in the modelling, which also might bias the simulation results.

The datasets produced generated in our study are the only available long-term and relatively high-precision discharge sequences for the upper Yangtze River, which includes 16 combinations of outputs of four hydrological models that were driven by four GCMs simulations. The Simulations of river discharge under the RCP scenarios with anthropogenic climate change and under the piControl scenario without human-induced climate change could provide support for research on climate change and climate change impacts in the upper Yangtze River basin in the period 1861-2299. Additionally, the simulations also provide clues regarding the extent to which human-induced climate change may impact streamflow in the upper Yangtze River. Simulations by multiple hydrological models and GCMs can provide a range of streamflow variations in future, which is a clue for water resource management strategies. According to our simulation results, the daily simulated discharge will be reduced with the decreasing precipitation in the future. Comparison of long-term simulated daily discharge under RCPs with anthropogenic climate change and under the piControl scenario without human-induced climate change can provide support to understand to which extent human-induced climate change may impact hydrological regime in the upper Yangtze River basin.

Author contribution

Chao Gao, Buda Su, Qianyu Zha, Cai Chen and Gang Luo run the hydrological models. Chao Gao, Buda Su and Tong Jiang analysed results and draft the manuscript. Xiaofan Zeng, Jinlong Huang, Min Xiong and Liping Zhang assisted the data processing. Valentina Krysanova provided guidance for the calibration/validation of the models and the description of results. All authors reviewed the resulting inventory and assisted with paper writing.

Competing interests

The authors declare that they have no conflict of interest.

Acknowledgements

This study was jointly supported by the National Key Research and Development Program of China MOST (2018FY10050001), the National Natural Science Foundation of China (41871024), the High-level Talent Recruitment Program of Ningbo University and the cooperation project between the Natural Science Foundation of China and the Pakistan Science Foundation (41661144027). The authors would like to thank the ISI-MIP project for providing the climate data that was used in this study.

References

Arnold, J. G., Srinivasan, R., Muttiah, R. S., and Williams, J. R.: Large area hydrologic modeling and assessment part I: model development, J Am Water Resour As, 34, 73-89, doi:10.1111/j.1752-1688.1998.tb05961.x, 1998.

Bergström, S. and Forsman, A.: Development of a conceptual deterministic rainfall-runoff model, Hydrol. Res., 4, 147-170, https://doi.org/10.2166/nh.1973.0012, 1973.

Braud, I., Roux, H., Anquetin, S., Maubourguet, M. M., Manus, C., Viallet, P., and Dartus, D.: The use of distributed hydrological models for the Gard 2002 flash flood event: analysis of associated hydrological processes, J. Hydrol., 394, 162-181, https://doi.org/10.1016/j.jhydrol.2010.03.033, 2010.

Changjiang Water Resources Commission of the Ministry of Water Resources: The flood and drought disasters in the Yangtze River Basin, China Water & Power Press, Beijing, China, 2002.

Chen, J., Gao, C., Zeng, X. F., Xiong, M., Wang, Y. J., Jing, C., Krysanova, V., Huang, J. L., Zhao, N., and Su, B. D.: Assessing changes of river discharge under global warming of 1.5°C and 2°C in the upper reaches of the Yangtze River Basin: Approach by using multiple- GCMs and hydrological models, Quat. Int., 453, 63-73, https://doi.org/10.1016/j.quaint.2017.01.017, 2017.

Cheng, X. G., Zhang, J., and Gong, H. L.: HSPF hydrologic simulation and parameter uncertainty in a semi-arid and semi-humid area, Acta Scientiae Circumstantiae, 34, 3179-3187, 2014.

Dahl, T. A., Kendall A. D., and Hyndman, D. W.: Impacts of Projected Climate Change on Sediment Yield and Dredging Costs, Hydrol. Process., 32, 1223-1234, https://doi.org/10.1002/hyp.11486, 2018.

Dufresne, J. L., Foujols, M. A., Denvil, S., Caubel, A., Marti, O., Aumont, O., Balkanski, Y., Bekki, S., Bellenger, H., Benshila, R., Bony, S., Bopp, L., Braconnot, P., Brockmann, P., Cadule, P., Cheruy, F., Codron, F., Cozic, A., Cugnet, D., de Noblet, N., Duvel, J. P., Ethe, C., Fairhead, L., Fichefet, T., Flavoni, S., Friedlingstein, P., Grandpeix, J. Y., Guez, L., Guilyardi, E., Hauglustaine, D., Hourdin, F., Idelkadi, A., Ghattas, J., Joussaume, S., Kageyama, M., Krinner, G., Labetoulle, S., Lahellec, A., Lefebvre, M. P., Lefevre, F., Levy, C., Li, Z. X., Lloyd, J., Lott, F., Madec, G., Mancip, M., Marchand, M., Masson, S., Meurdesoif, Y., Mignot, J., Musat, I., Parouty, S., Polcher, J., Rio, C., Schulz, M., Swingedouw, D., Szopa, S., Talandier, C., Terray, P., Viovy, N., and Vuichard, N.: Climate change projections using the IPSL-CM5 Earth System Model: from CMIP3 to CMIP5, Clim. Dyn., 40, 2123-2165, https://doi.org/10.1007/s00382-012-1636-1, 2013.

Frieler, K., Lange, S., Piontek, F., Reyer, C. P. O., Schewe, J., Warszawski, L., Zhao, F., Chini, L., Denvil, S., Emanuel, K., Geiger, T., Halladay, K., Hurtt, G., Mengel, M., Murakami, D., Ostberg, S., Popp, A., Riva, R., Stevanovic, M., Suzuki, T., Volkholz, J., Burke, E., Ciais, P., Ebi, K., Eddy, T. D., Elliott, J., Galbraith, E., Gosling, S. N., Hattermann, F., Hickler, T., Hinkel, J., Hof, C., Huber, V., Jägermeyr, J., Krysanova, V., Marcé, R., Schmied, H. M., Mouratiadou, I., Pierson, D., Tittensor, D. P., Vautard, R., Vliet, M., Biber, M. F., Betts, R. A., Bodirsky, B. L., Deryng, D., Frolking, S., Jones, C. D., Lotze, H. K., Lotze-Campen, H., Sahajpal, R., Thonicke, K., Tian, H. Q., and Yamagata, Y.: Assessing the impacts of 1.5 °C global warming – simulation protocol of the Inter-Sectoral Impact Model Intercomparison Project (ISIMIP2b), Geosci. Model Dev., 10, 4321-4345, https://doi.org/10.5194/gmd-10-4321-2017, 2017.

Gao, C., Su, B.D., Krysanova V., Zha Q.Y., Chen C., Luo G., Zeng X.F., Huang J.L., Xiong M., Zhang L.P, Jiang T.: A 439-year daily discharge dataset (1861-2299) for the upper Yangtze River, China. 4TU.ResearchData, https://doi.org/10.4121/uuid:8658b22a-8f98-4043-9f8f-d77684d58cbc, 2019.

Gerhard, K. and Flanner, M. G.: Striking stationarity of large-scale climate model bias patterns under strong climate change, Proc. Natl. Acad. Sci. U. S. A., 115, 9462-9466, https://doi.org/10.1073/pnas.1807912115, 2018.

Gupta, H. V., Kling, H., Yilmaz, K. K., and Martinez, G. F.: Decomposition of the mean squared error and NSE performance criteria: implications for improving hydrological modelling, J. Hydrol., 377, 80-91, https://doi.org/10.1016/j.jhydrol.2009.08.003, 2009.

Hattermann, F. F., Krysanova, V., Gosling, S. N., Dankers, R., Daggupati, P., Donnelly, C., Floerke, M., Huang, S., Motovilov, Y., Buda, S., Yang, T., Mueller, C., Leng, G., Tang, Q., Portmann, F. T., Hagemann, S., Gerten, D., Wada, Y., Masaki, Y., Alemayehu, T., Satoh, Y., and Samaniego, L.: Cross-scale intercomparison of climate change impacts simulated by regional and global hydrological models in eleven large river basins, Clim. Change, 141, 561-576, https://doi.org/10.1007/s10584-016-1829-4, 2017.

Hu, M.S. and Luo, C.Z: The historical flood of China, China Bookstore press, Beijing, China, 1992.

Huang, J. L., Wang, Y. J., Su, B., and Zhai, J. Q.: Future Climate Change and Its Impact on Runoff in the Upper Reaches of the Yangze River Under RCP4.5 Scenario, Meteorological Monthly, 42, 614-620, https://doi.org/10.7519/j.issn.1000-0526.2016.05.011, 2016.

Jones, C. D., Hughes, J. K., Bellouin, N., Hardiman, S. C., Jones, G. S., Knight, J., Liddicoat, S., O'Connor, F. M., Andres, R. J., Bell, C., Boo, K. O., Bozzo, A., Butchart, N., Cadule, P., Corbin, K. D., Doutriaux-Boucher, M., Friedlingstein, P., Gornall, J., Gray, L., Halloran, P. R., Hurtt, G., Ingram, W. J., Lamarque, J. F., Law, R. M., Meinshausen, M., Osprey, S., Palin, E. J., Chini, L. P., Raddatz, T., Sanderson, M. G., Sellar, A. A., Schurer, A., Valdes, P., Wood, N., Woodward, S., Yoshioka, M., and Zerroukat, M.: The HadGEM2-ES implementation of CMIP5 centennial simulations, Geosci. Model Dev., 4, 543-570, https://doi.org/10.5194/gmd-4-543-2011, 2011.

Jung, I. W., Chang, H., and Moradkhani, H.: Quantifying uncertainty in urban flooding analysis considering hydro-climatic projection and urban development effects, Hydrol. Earth Syst. Sci, 15, 617-633, http://doi.org/10.5194/hess-15-617-2011, 2011.

Krysanova V., Donnelly Ch., Gelfan A., Gerten D., Arheimer B., Hattermann F., and Kundzewicz Z.: How the performance of hydrological models relates to credibility of projections under climate change, Hydrolog SCI J., 63, 696-720, https://doi.org/10.1080/02626667.2018.1446214, 2018.

Krysanova V., Hattermann F., and Wechsung F.: Development of the ecohydrological model SWIM for regional impact studies and vulnerability assessment, Hydrol. Process, 19, 763–783, https://doi.org/10.1002/hyp.5619, 2005.

Lai, C., Reinders, M. J. T., and Wessels, L.: Random subspace method for multivariate feature selection, Pattern. Recogn. Lett., 27, 1067-1076, https://doi.org/10.1016/j.patrec.2005.12.018, 2006.

Lange, S.: Bias correction of surface downwelling longwave and shortwave radiation for the EWEMBI dataset, Earth. Syst. Dynam., 9, 627-645, https://doi.org/10.5194/esd-2017-81, 2018.

Liang, X., Lettenmaier, D. P., Wood, E. F., and Burges, S. J.: A simple hydrologically based model of land surface water and energy fluxes for general circulation models, J. Geophys. Res.-Atmos., 99, 14415–14428, https://doi.org/10.1029/94JD00483, 1994.

Longfield, S. A., Faulkner, D., Kjeldsen, T. R., Macklin, M. G., Jones, A. F., Foulds, S. A., Brewer, P. A., Griffiths, H. M.: Incorporating sedimentological data in UK flood frequency estimation, J. Flood Risk Manag., e12449, https://doi.org/10.1111/jfr3.12449, 2018.

Luo, C.Z. and Le, J.X: The flood of China, China Bookstore press, Beijing, China, 1996.

Maisa, R., Fabrice, L., Julian, R. V., and Andrew, J. C.: Emergence of robust precipitation changes across crop production areas in the 21st century, Proc. Natl. Acad. Sci. U. S. A., 116, 6673-6678, https://doi.org/10.1073/pnas.1811463116, 2019.

Meaurio, M., Zabaleta, A., Boithias, L., Epelde, A. M., Sauvage, S., Sanchez-Perez, J. M., Srinivasan, R., and Autiguedad, I: Assessing the hydrological response from an ensemble of CMIP5 climate projections in the transition zone of the Atlantic region (Bay of Biscay), J. Hydrol., 548, 46-62, https://doi.org/10.1016/j.jhydrol.2017.02.029, 2017.

Miralles, D. G., Holmes, T. R. H., De, J. R. A. M., Gash, J. H., Meesters, A. G. C. A., and Dolman, A. J.: Global land-surface evaporation estimated from satellite-based observations, Hydrol. Earth Syst. Sci., 15, 453-469, https://doi.org/10.5194/hess-15-453-2011, 2011

Moriasi, D. N., Arnold, J. G., Van Liew, M. W., Bingner, R. L., Harmel, R. D., and Veith, T. L.: Model evaluation guidelines for systematic quantification of accuracy in watershed simulations, T. Asabe, 50, 885-900, https://doi.org/10.13031/2013.23153, 2007.

Nash, J. E., and Sutcliffe, J. V.: River flow forecasting through conceptual models part I — A discussion of principles, J. Hydrol., 10, 282-290, https://doi.org/10.1016/0022-1694(70)90255-6, 1970.

Raman Vinna, L., Wuest, A., Zappa, M., Fink, G., and Bouffard, D.: Tributaries affect the thermal response of lakes to climate change, Hydrol. Earth Syst. Sci., 22, 1-40, https://doi.org/10.5194/hess-22-31-2018, 2018.

Ren, Z. H., Zhao, P., Zhang, Q., Zhang, Z. F., Cao, L. J., Yang, Y. R., Zou, F. L., Zhao, Y. F., Zhao, H. M., Chen, Z.: Quality control procedures for hourly precipitation data from automatic weather stations in China, Meteorological Monthly, 36, 123–132, https://doi.org/10.3788/HPLPB20102207.1462,2010. (in Chinese)

Seneviratne, S. I., Rogelj, J., Seferian, R., Wartenburger, R., Allen, M. R., Cain, M., Millar, R. J., Ebi, K. L., Ellis, N., Hoegh-Guldberg, O., Payne, A. J., Schleussner, C. F., Tschakert, P., Warren, R. F.: The many possible climates from the Paris Agreement's aim of 1.5 degrees C warming, Nature, 558, 41-49, https://doi.org/10.1038/s41586-018-0181-4, 2018.

Stagl, J. C. and Hattermann, F. F.: Impacts of climate change on riverine ecosystems: Alterations of ecologically relevant flow dynamics in the danube river and its major tributaries, Water, 8, 566, https://doi.org/10.3390/w8120566, 2016.

Su, B., Gemmer, M., and Jiang, T.: Spatial and temporal variation of extreme precipitation over the Yangtze River Basin, Quat. Int., 186, 22-31, https://doi.org/10.1016/J.QUAINT.2007.09.001, 2008.

Su, B., Huang, J. L., Zeng, X. L., Gao, C., and Jiang, T.: Impacts of climate change on streamflow in the upper Yangtze River basin, Clim. Change, 141, 533-546, https://doi.org/10.1007/s10584-016-1852-5, 2017.

Su, B., Zeng X. F., Zhai, J. Q., Wang, Y. J., and Li, X. C.: Projected precipitation and streamflow under SRES and RCP emission scenarios in the Songhuajiang River basin, China, Quat. Int., 380, 95-105, https://doi.org/10.1016/j.quaint.2014.03.049, 2015.

Taylor, K. E., Stouffer R. J., and Meehl G. A.: An Overview of CMIP5 and the Experiment Design, B. Am. Meteorol. Soc., 93, 485-498, https://doi.org/10.1175/BAMS-D-11-00094.1, 2012.

Thomas, F., Marco, G., Liu, L., Su, B.: Change-points in climate extremes in the Zhujiang River Basin, South China, 1961–2007, J. Clim., 110: 783-799, https://doi.org/10.1007/s10584-011-0123-8, 2012.

Wang, G. J., Jiang, T., Blender, R., and Fraedrich, K.: Yangtze 1/f discharge variability and the interacting river–lake system, J. Hydrol., 351, 230-237, https://doi.org/10.1016/j.jhydrol.2007.12.016, 2008.

Watanabe, M., Suzuki, T., O'ishi, R., Komuro, Y., Watanabe, S., Emori, S., Takemura, T., Chikira, M., Ogura, T., Sekiguchi, M., Takata, K., Yamazaki, D., Yokohata, T., Nozawa, T., Hasumi, H., Tatebe, H., and Kimoto, M.: Improved climate simulation by MIROC5: mean states, variability, and climate sensitivity, J. Clim., 23, 6312-6335, https://doi.org/10.1175/2010JCLI3679.1, 2010.

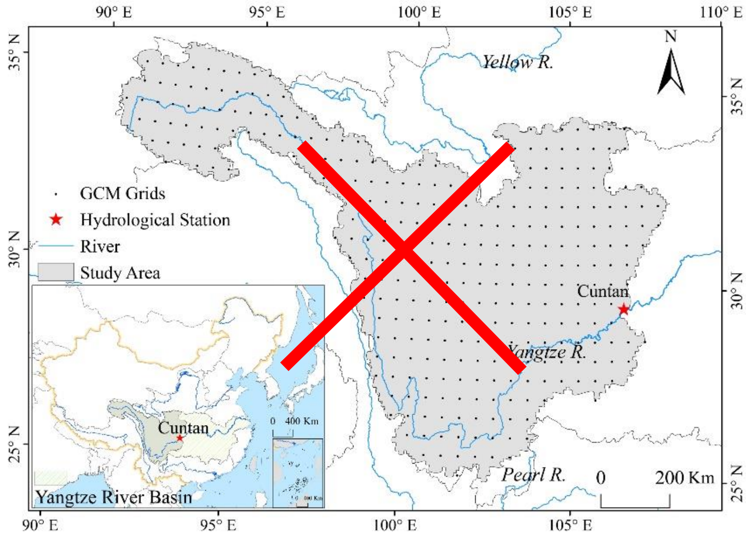

Figure 1: Location of the Cuntan hydrological station and the GCM grids in the upper Yangtze River basin

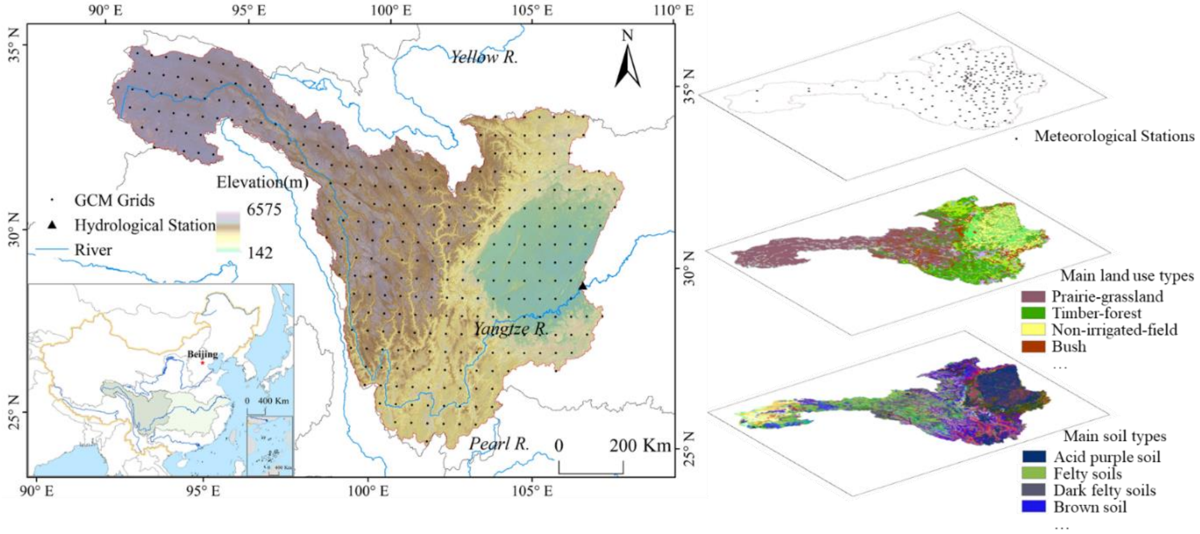

Figure 1 Location of the Cuntan hydrological station, GCM grids, meteorological stations and spatial distribution of the land use and soil types in the upper Yangtze River basin

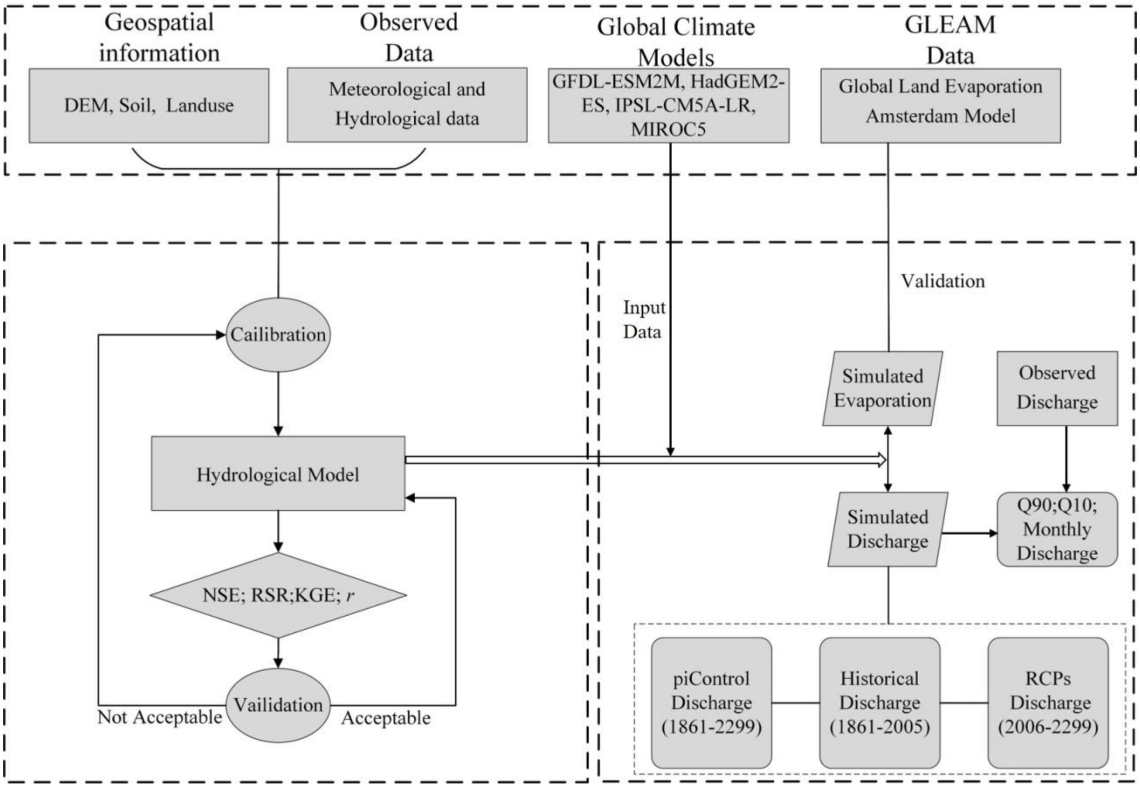

Figure 2 Flowchart for hydrological modelling process

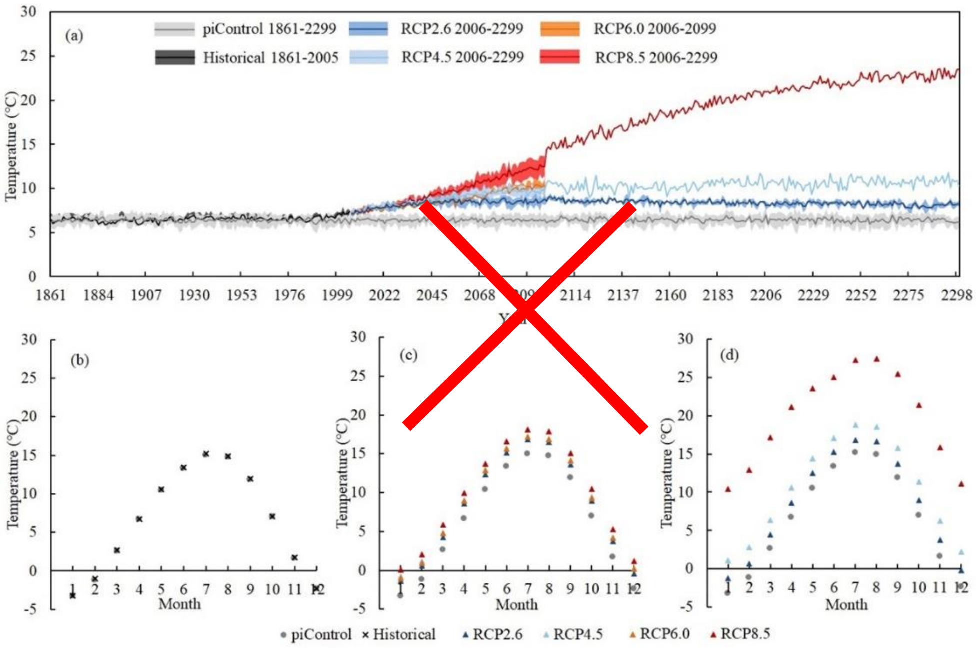

~~Figure 2: Interannual (a) and long-term average seasonal (b-d) dynamics of the surface air temperature in the upper Yangtze basin: comparison of the piControl scenario with the historical and anthropogenic climate change RCP scenarios (periods: a: 1861-2299; b: 1861-2005; c: 2006-2099; and d: 2100-2299)~~

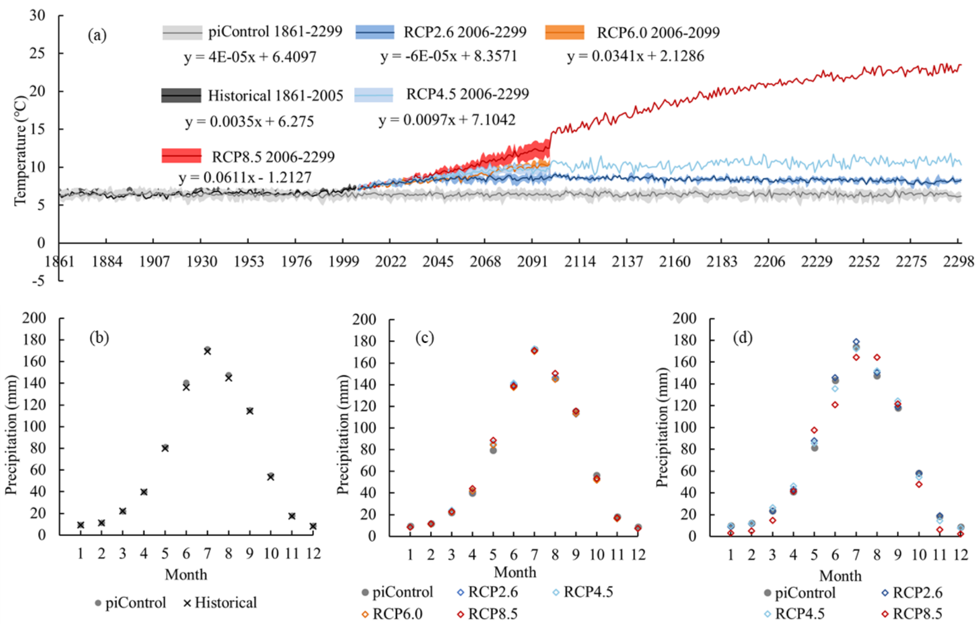

Figure 3 Inter-annual (a) and long-term averaged monthly dynamics (b-d) of the surface air temperature in the upper Yangtze River basin: comparison of the piControl scenario with the anthropogenic climate change scenarios (periods: a: 1861 - 2299; b: 1861 - 2005; c: 2006 - 2099; and d: 2100 - 2299)

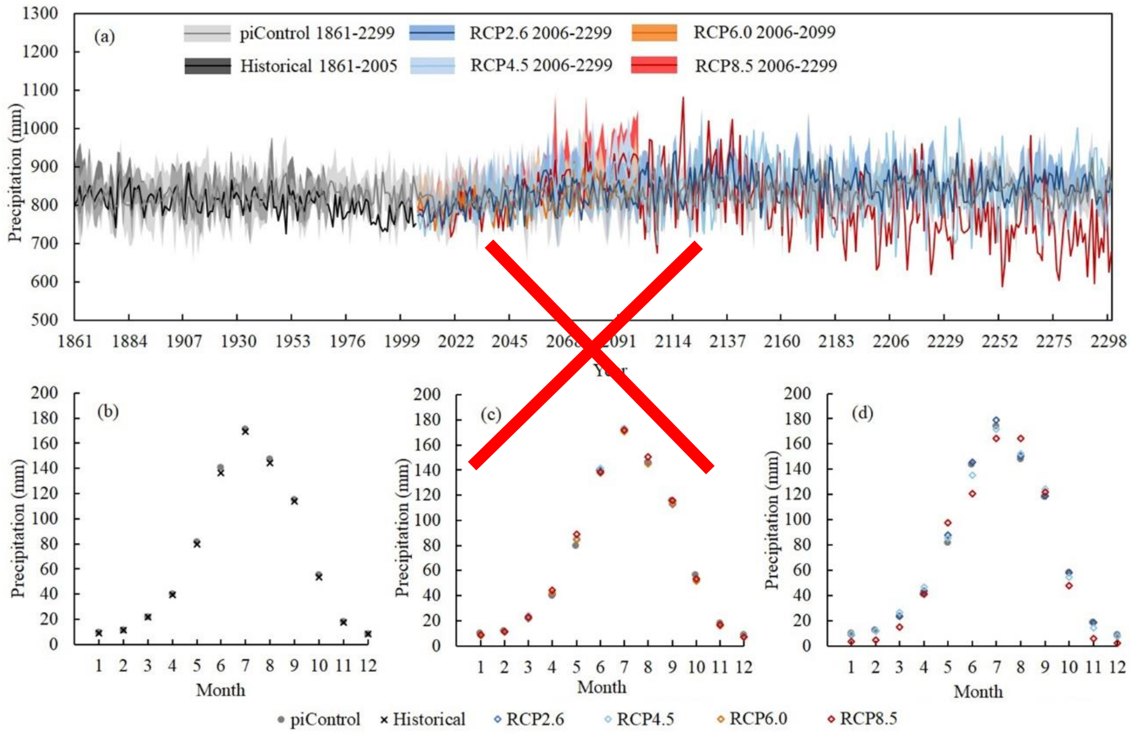

~~**Figure 3: Annual (a) and long-term average seasonal (b-d) dynamics of precipitation in the upper Yangtze basin: comparison of the piControl scenario with the historical and anthropogenic climate change RCP scenarios (periods: a: 1861-2299; b: 1861-2005; c: 2006-2099; and d: 2100-2299)**~~

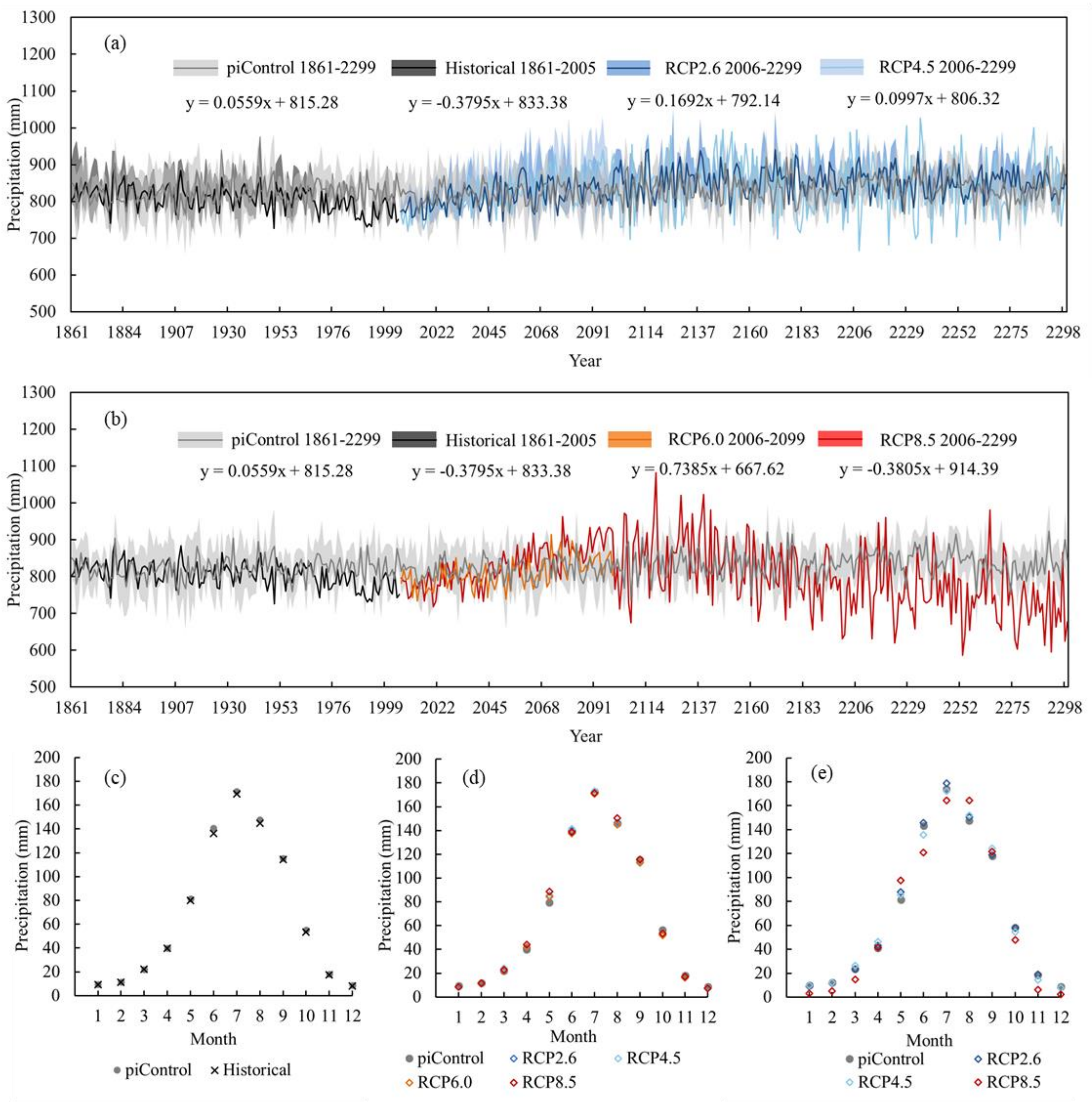

Figure 4 Inter-annual (a-b) and long-term averaged monthly dynamics (c-e) of precipitation in the upper Yangtze River basin: comparison of the piControl scenario with the anthropogenic climate change scenarios (periods: a: 1861-2299; b: 1861-2299; c: 1861 - 2005; d: 2006 - 2099; and e: 2100 - 2299)

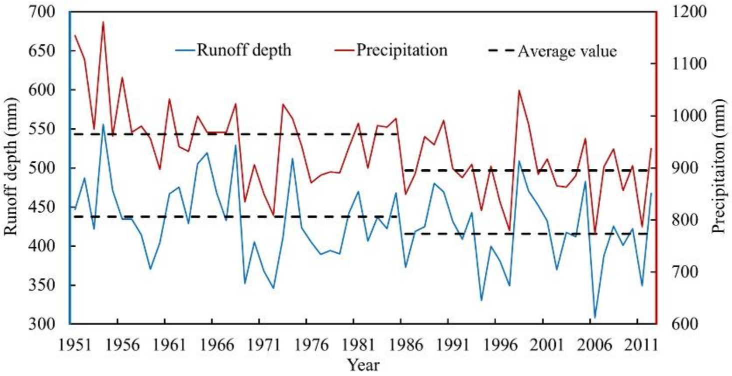

~~Figure 4~~ Figure 5 **Annual precipitation and runoff depth observed in the upper Yangtze River basin in the period 1951 - 2012**

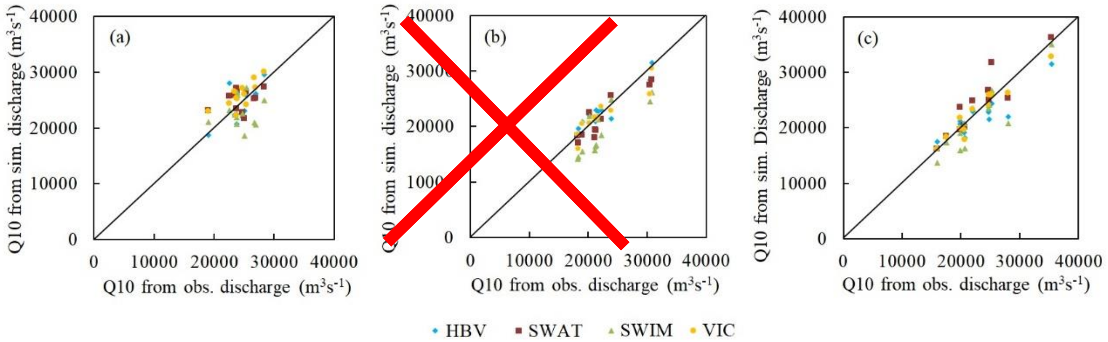

~~Figure 5: Comparison of the Q10 values based on the simulated and observed discharge data at the Cuntan station in the calibration period, 1979-1990, (a) and validation periods, 1967-1978 (b) and 1991-2002 (c)~~

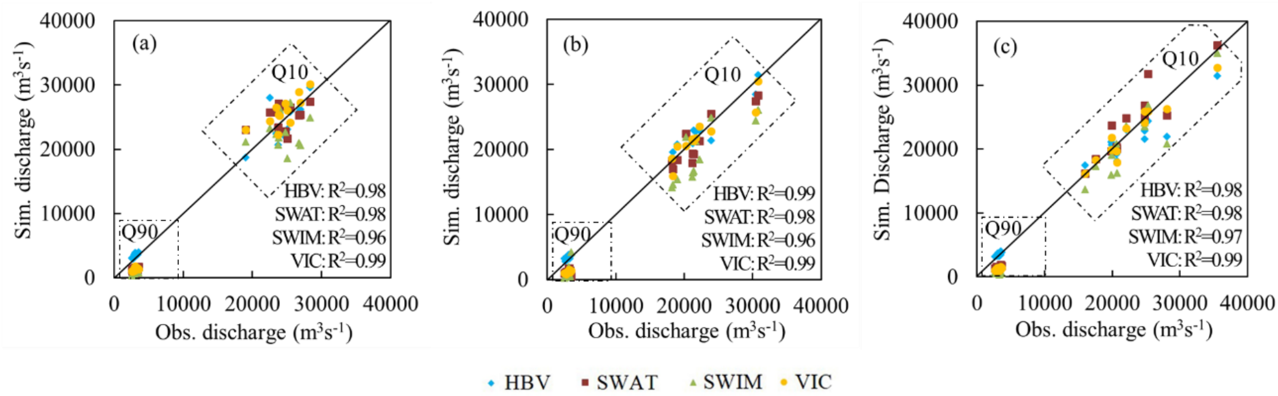

Figure 6 Comparison of the simulated and observed Q10, Q90 percentiles at the Cuntan station in the calibration period 1979 - 1990 (a) and validation period 1967 - 1978 and 1991 - 2002 (b-c)

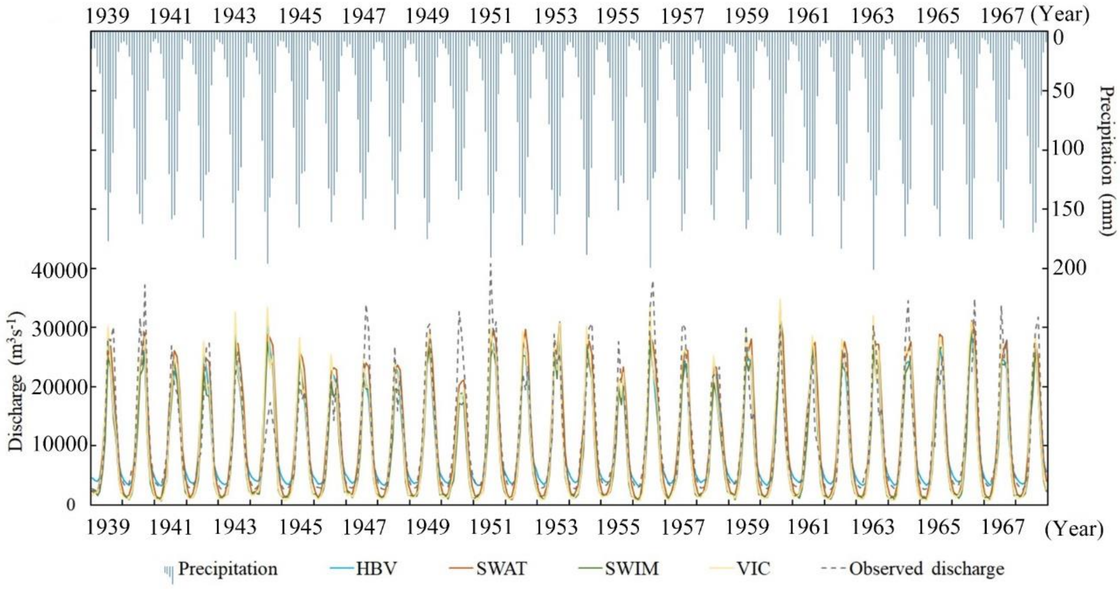

~~Figure 6~~ Figure 7 **Observed and simulated monthly discharge and precipitation at the Cuntan station in the upper Yangtze basin in the period 1939 - 1968**

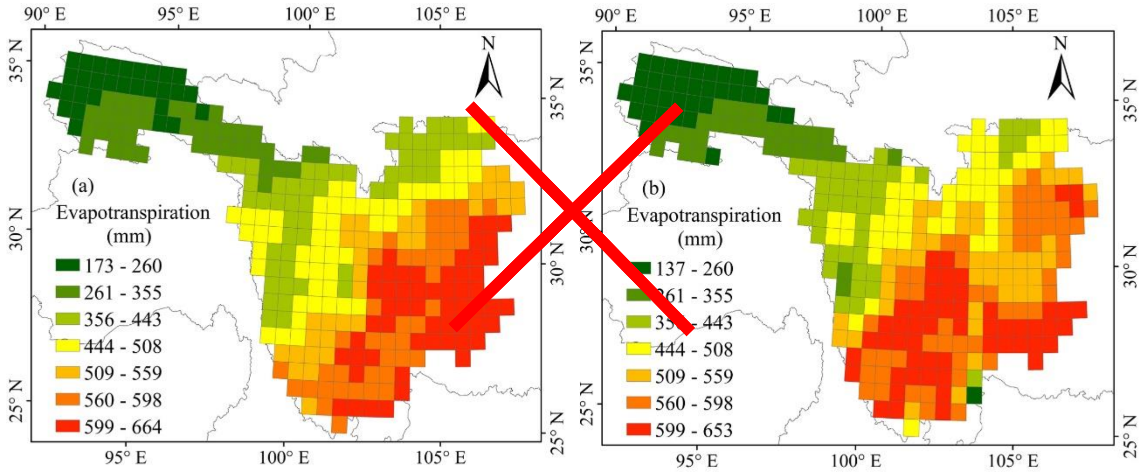

~~Figure 7: Spatial distribution of the mean annual evapotranspiration in the upper Yangtze River basin in the period 1986-2005 based on outputs from the hydrological model VIC (a) and GLEAM (b)~~

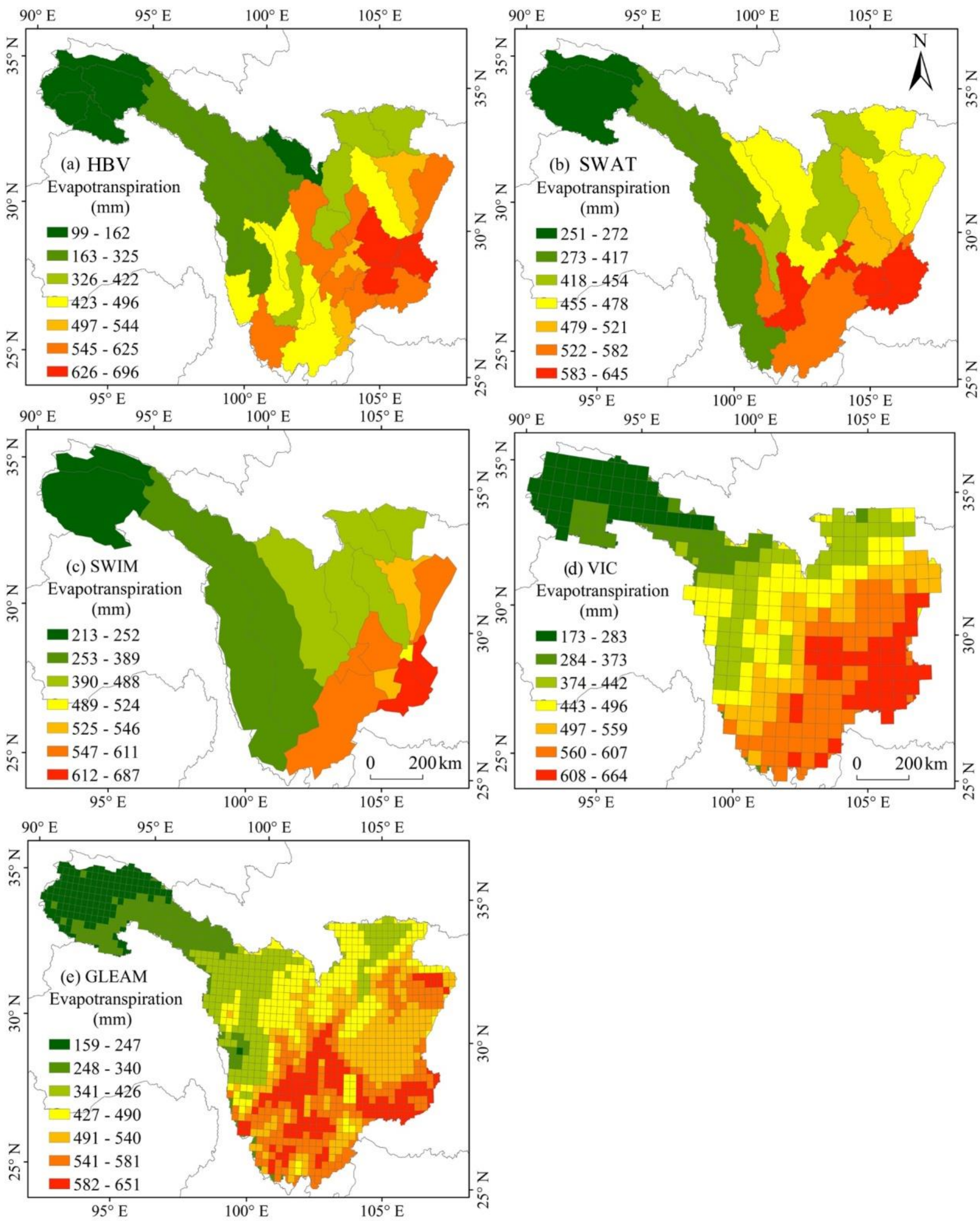

Figure 8 Spatial distribution of multi-year averaged annual evapotranspiration in the upper Yangtze River basin for 1986 - 2005: HBV output (a), SWAT output (b), VIC output (c), SWIM output (d) and GLEAM data(e)

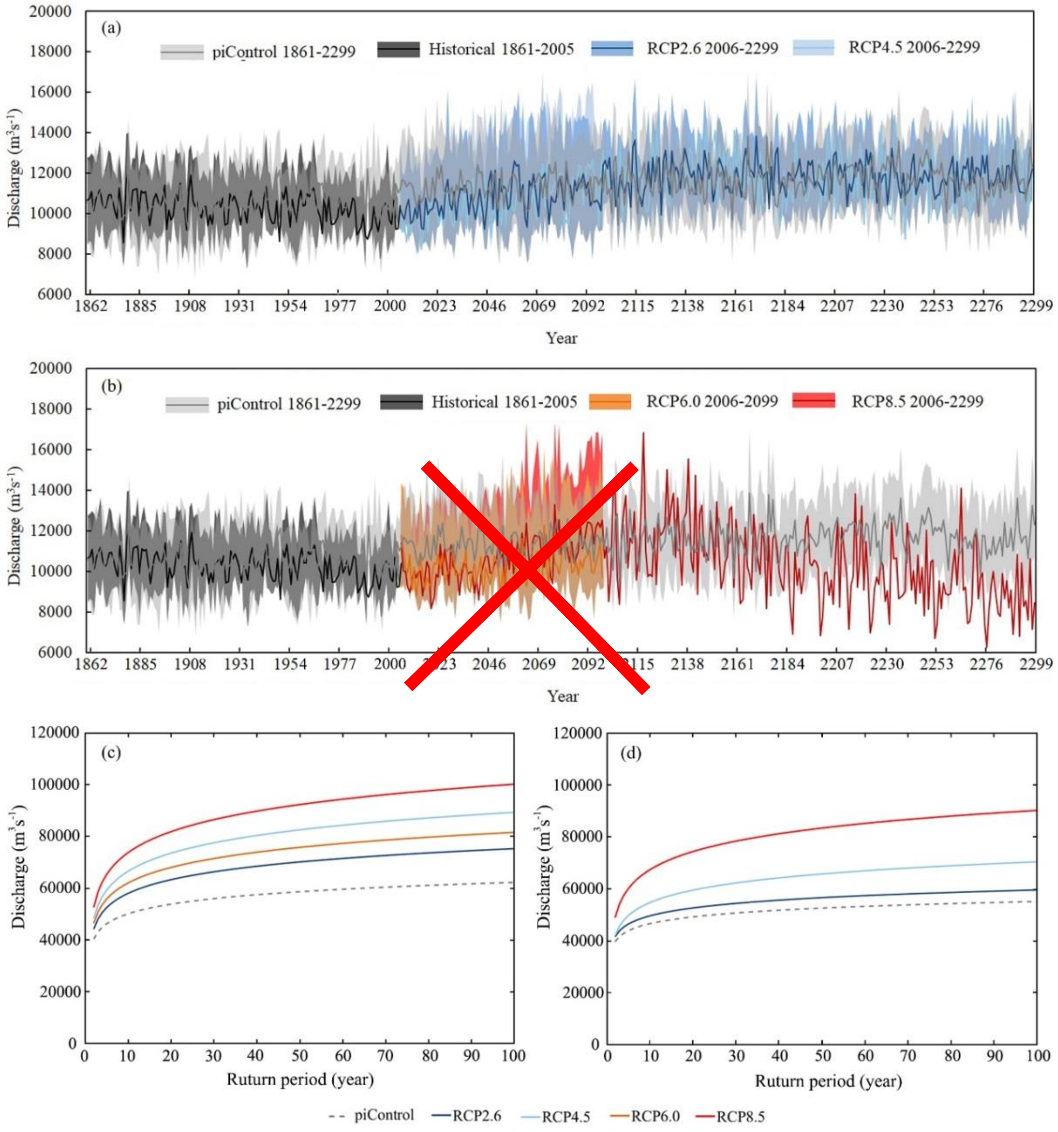

~~**Figure 8: The annual mean discharge under the piControl scenario and scenarios with anthropogenic climate change effects simulated by the four hydrological models (SWIM, SWAT, HBV, and VIC) (a-b) and the return periods of daily maximum discharge (c-d) at the Cuntan station; comparison of the piControl scenario with the anthropogenic climate change RCP scenarios (periods: a-b: 1861-2299; c: 2070-2099; and d: 2170-2199)**~~

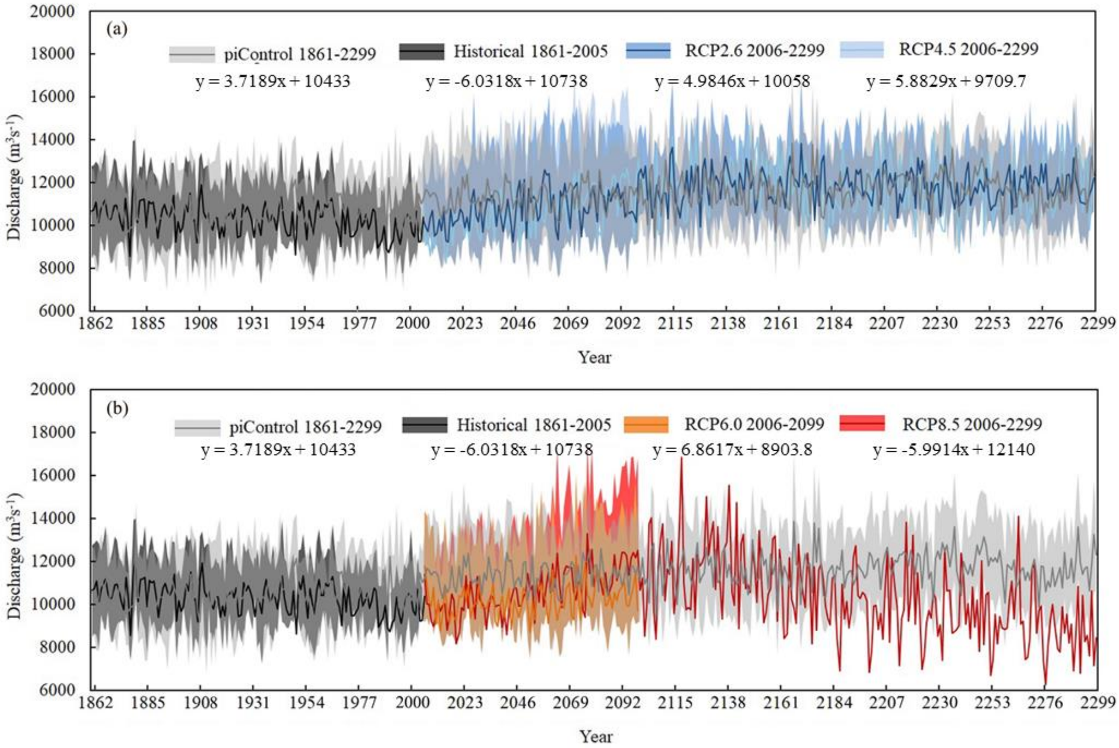

Figure 9 The annual mean discharge at the Cuntan station simulated by four hydrological models (HBV, SWAT, SWIM, and VIC) under the piControl scenario and scenarios with anthropogenic climate change effects (a-b)

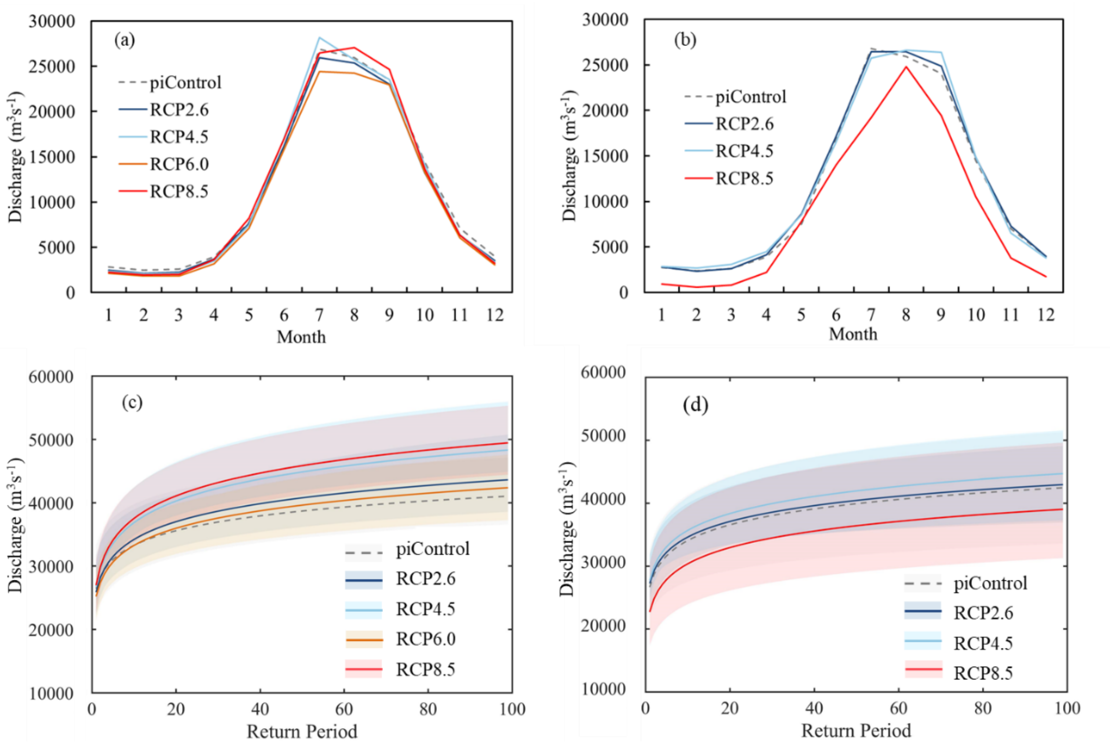

Figure 10 Comparison of monthly mean simulated discharge and return periods of daily maximum discharge at the Cuntan station for 2070 - 2099 (a, c) and 2270 - 2299 (b, d) under RCPs and the piControl scenario

Table 1 Availability of climate scenarios from four climate models for different periods

Climate scenario	CO_2 concentration	GFDL-ESM2M	HadGEM2-ES	IPSL-CM5A-LR	MIROC5
piControl scenario	286 ppm	1861-2099	1861-2299	1861-2299	1861-2299
Historical scenario	Recorded CO_2	1861-2005	1861-2005	1861-2005	1861-2005
Future scenario	RCP2.6	2006-2099	2006-2299	2006-2299	2006-2299
	RCP4.5	2006-2099	2006-2099	2006-2299	2006-2099
	RCP6.0	2006-2099	2006-2099	2006-2099	2006-2099
	RCP8.5	2006-2099	2006-2099	2006-2299	2006-2099

Table 2 Short description of HBV, SWAT, SWIM, and VIC

Model	Developed Institution	Spatial disaggregation	Representation of soils	Representation of vegetation	Routing method
HBV	Swedish Meteorological and Hydrological Institution	Sub-basins, 10 elevation zones & land use classes	1 soil layer, 2 soil parameters	Fixed monthly plant characteristics	A simple time-lag method
SWAT	United States Department of Agriculture	Sub-basins and hydrological response units	Up to 10 soil layers, 11 soil parameters	A simplified EPIC approach	Muskingum method
SWIM	The Potsdam Institute for Climate Impact Research, based on the SWAT and MATSALU models	Sub-basins and hydrotopes	Up to 10 soil layers, 11 soil parameters	A simplified EPIC approach	Muskingum method, reservoirs and irrigation
VIC	University of Washington, University of California, and Princeton University	Grid of large and uniform cells with sub-grid heterogeneity	3 soil layers, 19 parameters	Fixed monthly plant characteristics	Linearized St. Venant's equations

Table 3 The parameters and their ranges used for calibration of four hydrological models

HBV Name	Range	SWAT Name	Range	SWIM Name	Range	VIC Name	Range
Threshold quick runoff (UZ1)	0-100	Deep aquifer percolation fraction (*Rchrg_Dp*)	0-1	Routing coefficient 1 (*roc1*)	1-100	Non-linear baseflow begins (*Ds*)	0-1
Percolation to lower zone (*PREC*)	0-6	Saturated hydraulic conductivity (*Sol_K*)	0-100	Routing coefficient 2 (*roc2*)	1-100	Maximum baseflow (Ds_{max})	0-30
Non-linearity in soil water zone (*BETA*)	1-5	Maximum canopy storage (*Canmx*)	0-10	Evaporation coefficient (*thc*)	0.5-1.5	Maximum soil moisture (*Ws*)	0-1
Slow time constant upper zone (*KUZ1*)	0.01-1	Average slope steepness (*Slope*)	0-0.6	Baseflow factor for return flow travel time (*bff*)	0.2-1	Variable Infiltration Capacity curve (b_i)	0-0.4
Additional precipitation coefficient for snow at gauge (*SKORR*)	1-3	Available water capacity (*Sol_Awc*)	0-1	Coefficient to correct channel width (*chwc0*)	0.1-1	Soil depth 1 (d_1)	0.1-1
Precipitation correction for rain (*PKORR*)	0.8-3	Initial SCS CN II value (*Cn2*)	35-98	Saturated conductivity (*sccor*)	0.01-10	Soil depth 2 (d_2)	0.1-2
		Groundwater "revap" coefficient (*Gw_Revap*)	0.02-0.2	Groundwater recession rate (*abf*)	0.01-1	Soil depth 3 (d_3)	0.1-3
		Biological mixing efficiency (*Biomix*)	0-1	Initial conditions (*gwq0*)	0.01-1		
		Soil evaporation compensation factor (*Esco*)	0-1	Curve number (*cnum*)	10-100		

~~Table 3: Evaluation criteria for testing performance of hydrological models~~

Criterion	Formula	Range	Ideal value	Notation
Nash-Sutcliffe efficiency (NSE)	$1-\frac{\sum_{t=1}^{N}\left(Q_{s,t}-Q_{o,t}\right)^{2}}{\sum_{t=1}^{N}\left(Q_{o,t}-\bar{Q}_{o}\right)^{2}}$	(-∞, 1)	1	Q_s: simulated discharge; Q_o: observed discharge; $\bar{Q}_o$: mean of observed discharge;
Ratio of the root mean square error and the standard deviation of observation (RSR)	$\frac{\sqrt{\sum_{t=1}^{N}\left(Q_{o,t}-Q_{s,t}\right)^{2}}}{\sqrt{\sum_{t=1}^{N}\left(Q_{o,t}-\bar{Q}_{o}\right)^{2}}}$	(0, +∞)	0	$\bar{Q}_s$: mean of simulated discharge; t: sequence of the discharge series;
Pearson's correlation coefficient (r)	$\frac{\sum_{t=1}^{N}\left(Q_{s,t}-\bar{Q}_{s}\right)\left(Q_{o,t}-\bar{Q}_{o}\right)}{\sqrt{\sum_{t=1}^{N}\left(Q_{s,t}-\bar{Q}_{s}\right)^{2}}-\sqrt{\sum_{t=1}^{N}\left(Q_{o,t}-\bar{Q}_{o}\right)^{2}}}$	(-1, 1)	1	N: number of time steps;
Modified Kling -Gupta efficiency (KGE)	$1-\sqrt{(\alpha-1)^{2}+(\beta-1)^{2}+(r-1)^{2}}$	(-∞, 1)	1	α: ratio between the standard deviations of the simulated and observed data; β: ratio between the mean simulated and mean observed discharge

Table 4 Evaluation criteria for testing simulation capacity of hydrological models

Criterion	Formula	Range	Ideal value	Notation	Reference
Nash-Sutcliffe efficiency (NSE)	$1-\frac{\sum_{t=1}^{N}\left(Q_{s,t}-Q_{o,t}\right)^2}{\sum_{t=1}^{N}\left(Q_{o,t}-\bar{Q}_o\right)^2}$	(-∞, 1)	1	Q_s: simulated discharge; Q_o: observed discharge;	(Nash and Sutcliffe, 1970)
Ratio of the root mean square error and the standard deviation of observation (RSR)	$\frac{\sqrt{\sum_{t=1}^{N}\left(Q_{o,t}-Q_{s,t}\right)^2}}{\sqrt{\sum_{t=1}^{N}\left(Q_{o,t}-\bar{Q}_o\right)^2}}$	(0, +∞)	0	$\bar{Q}_o$: mean of observed discharge; $\bar{Q}_s$: mean of simulated discharge;	(Moriasi et al., 2007)
Pearson's correlation coefficient (r)	$\frac{\sum_{t=1}^{N}\left(Q_{s,t}-\bar{Q}_s\right)\left(Q_{o,t}-\bar{Q}_o\right)}{\sqrt{\sum_{t=1}^{N}\left(Q_{s,t}-\bar{Q}_s\right)^2}-\sqrt{\sum_{t=1}^{N}\left(Q_{o,t}\right.}}$	(-1, 1)	1	t: sequence of the discharge series;	(Huang et al., 2012)
Modified Kling -Gupta efficiency (KGE)	$1-\sqrt{(\alpha-1)^2+(\beta-1)^2+(r-1}$	(-∞, 1)	1	N: number of time steps; α: ratio between the standard deviations of the simulated and observed data; β: ratio between the mean simulated and mean observed discharge	(King et al., 2012)

Table 5 Mean values of temperature, precipitation and simulated discharge in different scenarios

		piControl scenario	Historical scenario	Future scenario			
				RCP2.6	RCP4.5	RCP6.0	RCP8.5
Temperature (°C)	1861-2005	6.40	6.53	-	-	-	-
	2006-2099	6.41	-	8.27	8.79	8.70	9.72
	2100-2299	6.43	-	8.38	10.48	-	19.94
Precipitation (mm)	1861-2005	821.8	805.7	-	-	-	-
	2006-2099	819.2	-	814.9	823.8	809.8	830.2
	2100-2299	835.7	-	854.2	841.0	-	790.4
Discharge (m^3s^{-1})	1861-2005	10578.0	10294.4	-	-	-	-
	2006-2099	11338.6	-	10784.6	10592.6	10224.6	10617.8
	2100-2299	11698.5	-	11859.2	11824.3	-	10279.2

~~**Table 4: Criteria of fit of the four hydrological models in the calibration period and in the wet and dry validation periods**~~

Table 6 Performance of four hydrological models in the upper Yangtze River at the calibration period and the wet and dry validation periods

Criterion	Threshold	Calibration/validation	HBV	SWAT	SWIM	VIC
NSE	>=0.7	1979-1990	0.86	0.81	0.75	0.89
		1967-1978 (wet period)	0.86	0.79	0.7	0.88
		1991-2002 (dry period)	0.86	0.81	0.75	0.89
RSR	<=0.6	1979 - 1990	0.39	0.43	0.50	0.33
		1967-1978 (wet period)	0.38	0.46	0.55	0.34
		1991-2002 (dry period)	0.36	0.42	0.48	0.32
r	>=0.9	1979-1990	0.92	0.91	0.91	0.97
		1967-1978 (wet period)	0.92	0.90	0.89	0.96
		1991-2002 (dry period)	0.94	0.92	0.93	0.97
KGE	>=0.7	1979-1990	0.87	0.9	0.7	0.71
		1967-1978 (wet period)	0.90	0.88	0.65	0.69
		1991-2002 (dry period)	0.85	0.89	0.56	0.68

Table 5: Comparison of changes in the mean annual discharge, Q10 and Q90 in the period 2006-2299 under the scenarios of anthropogenic climate change and the piControl scenario

Dataset	Rate of change (Mean) (%)	Rate of change (Q10) (%)	Rate of change (Q90) (%)	Standard deviation	Coefficient of variation
piControl	-	-	-	980.4	0.08
RCP2.6	-0.92	-0.49	-3.8	1146.2	0.10
RCP4.5	-4.7	5.2	-11.9	1819.6	0.17
RCP6.0	-7.7	-7.3	-7.9	965.9	0.09
RCP8.5	-18.2	-2.9	-30.6	2347.9	0.25

Table 7 Relative changes in mean annual discharge, Q10 and Q90 in the periods 2070 - 2099 and 2270 - 2299 under the scenarios of anthropogenic climate change relative to the piControl scenario

Period	Scenarios	Relative change of mean discharge (%)	Relative change of Q10 (%)	Relative change of Q90 (%)	Standard deviation	Coefficient of variation
2070-2099	piControl	-	-	-	607.1	0.05
	RCP2.6	-4.2	-1.2	-5.4	681.1	0.06
	RCP4.5	-1.1	3.2	-10.9	997.1	0.09
	RCP6.0	-9.1	-3.5	-10.6	763.7	0.07
	RCP8.5	-0.7	4.3	-3.5	917.3	0.08
2270-2299	piControl	-	-	-	767.6	0.06
	RCP2.6	2.2	2.5	3.2	608.8	0.05
	RCP4.5	2.6	6.6	-2.3	1255.9	0.11
	RCP6.0	-	-	-	-	-
	RCP8.5	-30.6	-13.2	-50.4	1397.4	0.16